

## Tripodal Molecular Propeller Perturbs Microtubule Dynamics: Indole acts as a Blade and Plays Crucial Role in Anticancer Activity

Surajit Barman,<sup>a</sup> Gaurav Das,<sup>ab</sup> Prasenjit Mondal,<sup>ab</sup> Krishnangsu Pradhan,<sup>a</sup> Batakrishna Jana,<sup>c</sup> Juhee Khan,<sup>a</sup> Abhijit Saha,<sup>a</sup> Chirantan Kar,<sup>a</sup> Surajit Ghosh<sup>ab\*</sup>

- Organic and Medicinal Chemistry Division, CSIR-Indian Institute of Chemical Biology, 4, Raja S. C. Mullick Road, Kolkata-700032, India
- Academy of Scientific & Innovative Research (AcSIR), CSIR-IICB Campus, 4, Raja S. C. Mullick Road, Kolkata-700032, India
- Department of Chemistry, UNIST, Ulsan 44919, Republic of Korea.

Correspondence author: [sghosh@iicb.res.in](mailto:sghosh@iicb.res.in)

### Materials and Methods:

**Reagents:** Cyanuric chloride, Tryptophan methyl ester, Valine methyl ester, Methionine methyl ester, Glycine methyl ester, Proline methyl ester, Thiazolyl Blue Tetrazolium Bromide (MTT), Kanamycin sulfate, Dulbecco's Modified Eagle's Medium (DMEM), Guanosine 5'-triphosphate sodium salt hydrate (GTP), 4, 6-diamidino-2-phenylindole (DAPI), Trypsin-EDTA solution, Colchicine, 5(6)-carboxyfluorescein, PIPES, Ethylene glyol-bi(2-aminoethyl ether)-*N,N,N',N'*-tetra acetic acid (EGTA), *N,N'*-Diisopropylcarbodiimide (DIC), 8-anilino-1-naphthalenesulfonic acid ammonium salt (ANS) and Cell culture grade DMSO were purchased from Sigma-Aldrich. Sodium chloride, Sodium hydrogen carbonate, Di-sodium hydrogen phosphate dihydrate, Potassium hydroxide, Magnesium chloride hexahydrate, Trifluoroacetic acid (TFA) and Potassium dihydrogen phosphate were purchased from Merck. Potassium chloride and Agarose were purchased from Fisher Scientific. Dimethyl sulfoxide, *N, N'*-Diisopropylethylamine (DIPEA), Ethyl acetate, Chloroform and Hexane were purchased from Spectrochem. Triton-X-100 was purchased from SRL. 2-[4-(2-Hydroxyethyl) piperazin-1-yl] ethanesulfonic acid (HEPES) and Horse Serum were purchased from Himedia. Penicillin-Streptomycin and Fetal bovine serum were purchased from Invitrogen. Anti-alpha Tubulin clone EP 1332Y, Anti-Tubulin Antibody, Anti-Cytochrome C Antibody, Rabbit monoclonal antibody, and Goat Anti-mouse IgG (H+L) fluorescein conjugate were purchased from Merck Millipore. Goat pab to Rb IgG (Cy3.5) ab 6941 polyclonal rabbit was purchased from Abcam. Bisbenzimidazole H 33258 (hoechst) was purchased from Calbiochem. Propidium iodide (PI), p53 (F-8) mouse monoclonal IgG, p21 (F-5) mouse monoclonal IgG were purchased from Santa Cruz Biotechnology and Annexin V apoptosis detection kit from BD Biosciences. HPLC-grade water and acetonitrile were purchased from J.T. Baker. All the deuterated solvents were purchased from Cambridge isotope. All compounds were used without further purification.

## Methods:

### Cell culture

Human lung cancer cell line (A549), Human breast cancer cell line (MCF7), Human cervical cancer cell line (HeLa), Melanoma cancer cell line (B16F10), Human lung fibroblast normal cell line (WI38), Mouse myoblast cell line (C2C12) and Human breast epithelial cell line (MCF10A) were purchased from NCCS, Pune (India). The cells were cultured in 5% CO<sub>2</sub> humidified atmosphere at 37 °C in Dulbecco Modified Eagle medium (DMEM) containing 10% FBS, Kanamycin sulfate (110 mg/L), Penicillin (50 units/mL), and Streptomycin (50 µg/mL).

### Protein purification

Tubulin was isolated from goat brain and purified by two cycle's polymerization and depolymerization procedure followed by storing at -80 °C using 10% glycerol as described before.<sup>1</sup>

### Conformational analysis

Geometry optimization of each of the W<sub>3</sub>T compound was performed in 4 steps using Spartan' 16<sup>2-5</sup> and Gaussian' 09<sup>6</sup> program as described below:

- First Step:** A conformational search has been performed applying molecular mechanics force field (MMFF) on 1000 most probable conformers.
- Second Step:** We picked 100 lowest energy conformers from the previous MMFF calculation. These conformers are further refined using semi-empirical calculation at PM6 level.
- Third Step:** Subsequently, we have picked 20 lowest energy conformers from the semi-empirical calculation. The equilibrium geometry of these conformers is optimized applying Hartree-Fock method at 3-21G level.
- Forth Step:** Finally, we have picked 5 lowest energy conformers from the Hartree-Fock calculation for DFT optimization using Gaussian '09 program at the B3LYP/6-31G (d) level. The three lowest energy structures obtained from DFT calculations of corresponding W<sub>3</sub>T was considered as final structures for docking studies.

### Docking study

Blind docking study were performed using the software Autodock-Vina version 1.1.2.<sup>7</sup> A 98×60×64 affinity grids were centered on the receptor tubulin [PDB ID: 1Z2B]<sup>8</sup> for docking of study.

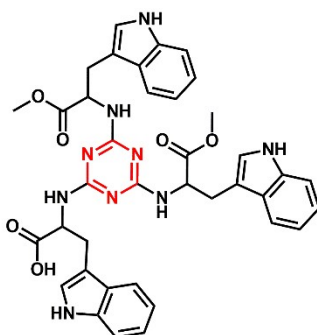
### Synthesis of 1, 3, 5-trisubstituted triazine derivatives

A solution of cyanuric chloride (2 mmol, 1 equivalents) and R<sub>1</sub>-NH<sub>2</sub> (8 mmol, 4 equivalents) in dry THF was stirred for 10 min. Then N, N'-diisopropylethylamine (3.5 mL) was added. The reaction mixture was refluxed overnight under nitrogen atmosphere. After the completion of reaction as indicated by TLC, the reaction was cooled down to room temperature. THF was removed by rotary evaporator. To this crude mixture, 10 mL of water was added and mixture was extracted with ethyl acetate (3 × 20 mL). The ethyl acetate layer was dried using anhydrous Na<sub>2</sub>SO<sub>4</sub> and evaporated in vacuum. Finally, the compounds were purified by column chromatography.

### Synthesis of fluorescein tagged of W<sub>3</sub>T

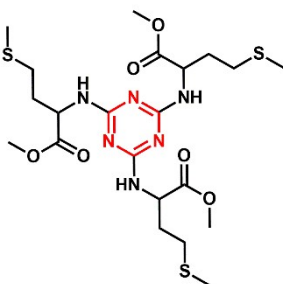
First, we performed the alkaline hydrolysis of W<sub>3</sub>T to make the acid derivatives W<sub>3</sub>T-COOH, using NaOH. The acid derivatives were coupled with Wang resin by CEM microwave peptide synthesizer (Liberty 1) for five minutes and microwave power was maintained 35 watt. N, N'-Diisopropylethylamine (DIPEA) and HBTU were used as an activator base and activator respectively in DMF. Next, ethylene diamine was coupled. Further, we have attached fluorescein to another free primary amine of diamine. In each step resin were washed by DMF, DCM and again DMF solvent successively. Finally, prepared fluorescein tagged molecule (F-W<sub>3</sub>T) was cleaved by TFA. Then, filtrate containing TFA was removed by nitrogen gas flow. All the prepared fluorescein attached molecules were purified through C-18 reverse phase HPLC column and mass were confirmed by MALDI-TOF in acetonitrile and water (1:1) mixture.

### Trimethyl 2,2',2''-((1,3,5-triazine-2,4,6-triyl)tris(azanediyl))tris(3-(1H-indol-3-yl)propanoate) (W<sub>3</sub>T):



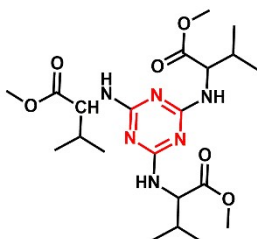
**<sup>1</sup>H NMR (300 MHz, Acetone-d<sub>6</sub>)** δ ppm: 3.21 - 3.36 (m, 6 H), 3.60 (s., 9 H), 4.87 (br. s., 3 H), 7.00 - 7.10 (m, 6 H), 7.20 (br. s., 3 H), 7.37 (d, *J*=8.05 Hz, 3 H), 7.56 (d, *J*=7.32 Hz, 3 H), 10.04 (br. s., 3 H). **<sup>13</sup>C NMR (75 MHz, CDCl<sub>3</sub>-d)** δ ppm: 27.42, 52.11, 54.02, 109.93, 111.24, 118.30, 119.08, 121.65, 123.62, 127.19, 136.03, 165.00, 173.81. **ESI-MS (Positive mode):** Expected mass for C<sub>39</sub>H<sub>39</sub>N<sub>9</sub>O<sub>6</sub> *m/z* is 730, found 730 (M), 731 (M + H<sup>+</sup>), 752 (M + Na<sup>+</sup>).

### Trimethyl 2,2',2''-((1,3,5-triazine-2,4,6-triyl)tris(azanediyl))tris(4-(methylthio) butanoate) (M<sub>3</sub>T):



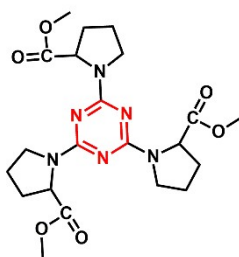
**<sup>1</sup>H NMR (300 MHz, CD<sub>3</sub>OD)** δ ppm 1.97 (br. s., 15 H) 2.40 - 2.53 (m, 6 H) 3.64 (s, 12 H) **<sup>13</sup>C NMR (150 MHz, CD<sub>3</sub>OD)** δ ppm 13.92, 29.40, 29.87, 31.14, 51.56, 52.61, 165.60, 174.38. **ESI-MS (Positive mode):** Expected mass for C<sub>21</sub>H<sub>36</sub>N<sub>6</sub>O<sub>6</sub>S<sub>3</sub> *m/z* is 565, found 565 (M), 587 (M + Na<sup>+</sup>), 603 (M + K<sup>+</sup>).

**Trimethyl 2,2',2''-((1,3,5-triazine-2,4,6-triyl)tris(azanediyl))tris(3-methyl butanoate) (V<sub>3</sub>T):**



**<sup>1</sup>H NMR (300 MHz, CDCl<sub>3</sub>)** δ ppm 0.88 (s, 9 H) 0.90(s, 9H) 2.03 - 2.14 (m, 3 H) 3.65 (s, 9 H) 4.47-4.51 (q, J=7.16 Hz, 3 H) **<sup>13</sup>C NMR (75 MHz, CDCl<sub>3</sub>)** δ ppm 18.42, 19.19, 30.86, 51.74, 58.72,165.92 , 173.99 **ESI-MS (Positive mode):** Expected mass for C<sub>21</sub>H<sub>36</sub>N<sub>6</sub>O<sub>6</sub> m/z is 468 (M), found 469 (M + H<sup>+</sup>), 491 (M + Na<sup>+</sup>).

**Trimethyl 1,1',1''-(1,3,5-triazine-2,4,6-triyl)tris(pyrrolidine-2-carboxylate) (P<sub>3</sub>T):**



**<sup>1</sup>H NMR (300 MHz, CD<sub>3</sub>OD)** δ ppm 1.89 - 2.04 (m, 9 H) 2.29 (br. s., 3 H) 3.45 - 3.61 (m, 3 H) 3.72 (s, 9 H) 4.24 - 4.48 (m, 3 H) 4.61 (s, 3 H). **<sup>13</sup>C NMR (150 MHz, CD<sub>3</sub>OD)** δ ppm 23.44, 23.60, 23.75, 29.81, 46.03, 51.14, 51.21, 58.67, 58.88, 59.08, 59.29, 78.12, 162.53, 163.04, 163.20, 163.55, 174.74, 175.20. **ESI-MS (Positive mode):** Expected mass for C<sub>21</sub>H<sub>36</sub>N<sub>6</sub>O<sub>6</sub>S<sub>3</sub> m/z is 463, found 463 (M), 585 (M + Na<sup>+</sup>).

**Trimethyl 2, 2', 2''-((1, 3, 5-triazine-2, 4, 6-triyl) tris (azanediyl)) triacetate (G<sub>3</sub>T):**



**<sup>1</sup>H NMR (300 MHz, METHANOL-d<sub>4</sub>)** δ ppm 3.60 (s, 9 H), 3.89-3.96 (br. Two singlet, 6H). **<sup>13</sup>C NMR (75 MHz, CD<sub>3</sub>OD)** δ ppm 41.842, 42.111, 51.328, 165.764, 172.013 **ESI-MS (Positive mode):** Expected mass for C<sub>12</sub>H<sub>18</sub>N<sub>6</sub>O<sub>6</sub> m/z is 342, found 343 (M + H<sup>+</sup>), 365 (M + Na<sup>+</sup>).

**Microtubule assembly assay**

Microtubule assembly assay was performed to understand whether triazine derivatives are interacting with tubulin or not. It was described before that fluorescence intensity of DAPI

increasing if there is formation of microtubule from tubulin which was examined by Fluorometer. A mixture of 10  $\mu\text{M}$  DAPI in BRB80 buffer containing 100  $\mu\text{M}$  tubulin, 10 mM GTP and different concentrations of triazine derivatives ( $\text{W}_3\text{T}$ ,  $\text{M}_3\text{T}$ ,  $\text{G}_3\text{T}$ ,  $\text{V}_3\text{T}$  and  $\text{P}_3\text{T}$ ) was added. First, we have performed this experiment with 100  $\mu\text{M}$  concentration of all the compounds. Then we used three different concentrations (25  $\mu\text{M}$ , 50  $\mu\text{M}$ , 100  $\mu\text{M}$ ) for the  $\text{W}_3\text{T}$ . After exciting at 355 nm wavelength at 37 °C and the emission spectra was recorded in region from 400 nm to 600 nm wavelength for 60 min in five min time interval in Quanta Master Spectrofluorometer (QM-40), which is equipped with Peltier for controlling the temperature during experiment. Control experiment was carried out under same condition in absence of tripodal compounds. The data was calculated in origin Pro 8.5 software.

### Determination of binding affinity of $\text{W}_3\text{T}$

Intrinsic tryptophan fluorescence intensity of tubulin is quenched when a small molecule binds with tubulin, which can be monitored by recording its fluorescence using fluorimeter. Here, tubulin (10  $\mu\text{M}$ ) was mixed with different concentration of  $\text{W}_3\text{T}$  compounds in BRB80 buffer and the mixture was incubated for 40 min at 25 °C. Then, solutions were excited at 295 nm and the data were recorded in the range 310-450 nm using Quanta Master spectrofluorimeter (QM-40) containing Peltier to maintain the fixed temperature. From all those data, binding constant was calculated using a modified Stern-Volmer equation. The data was calculated and plotted in origin Pro 8.5 software.

### SPR study

Surface plasmon resonance (SPR) <sup>9</sup> experiment was performed to determine association constant ( $K_a$ ) and dissociation constant ( $K_b$ ) of the  $\text{W}_3\text{T}$  along with a non-interacting compound (CP) with the tubulin. In this experiment, we used NTA biosensor chip surface and immobilized  $\text{Ni}^{2+}$  on the chip by flowing 500  $\mu\text{M}$   $\text{NiCl}_2$  solution over the surface. Streptavidin- $\text{His}_6$  solutions were flowed and immobilized it onto the surface as there is strong interaction of streptavidin- $\text{His}_6$  with the  $\text{Ni}^{2+}$ . After washing the surface with the running buffer, we flowed 20  $\mu\text{g/mL}$  biotinylated tubulin. Again, the surface was washed with running buffer and flowed the compound as an analyte with a flow rate of 30  $\mu\text{L/min}$ . The results were recorded and analyzed by plotting the curve with a local fitting by BIA evaluation software.

### Förster Resonance Energy Transfer (FRET) experiment between various Tubulin complexes and fluorescein tagged triazine compounds (F- $\text{W}_3\text{T}$ )

FRET is a photo physical process in which non-radiative energy is transferred from an excited donor molecule to an acceptor molecule. Now a days, FRET is very powerful technique to measure the accurate distance between two interacting molecules at angstrom distances (10-100 Å). Here, in this manuscript, we have applied this FRET to measure the distance of fluorescein attached  $\text{W}_3\text{T}$  molecule from various known binding location in the receptor tubulin and find out their exact binding site.

$$\text{Efficiency of FRET, } \epsilon_{\text{FRET}} = \frac{I_A}{\gamma I_D + I_A} \dots\dots\dots (1)$$

Where  $I_A$  and  $I_D$  are the intensity of acceptor and donor respectively and  $\gamma$  is a correction factor. The Forster distance ( $R_0$ ) between tubulin-colchicine complex and fluorescein-peptide is  $29.5 \pm 1$  Å, tubulin bound ANS and fluorescein-peptide is  $50.3 \pm 2$  Å and tubulin bound TAMRA-peptide with fluorescein-peptide is  $62.9 \pm 2$  Å. We have taken TAMRA-E3NAP peptide for FRET study

as it was well documented earlier that this peptide binds at the taxol binding site of  $\beta$  tubulin. Now, the distance ( $R_{DA}$ ) between various tubulin-complexes and F-W<sub>3</sub>T was calculated by the following equation.

$$R_{DA} = R_o \left( \frac{1 - \epsilon_{FRET}}{\epsilon_{FRET}} \right)^{\frac{1}{6}} \dots\dots\dots (2)$$

In our FRET studies, as obtained from Figure 2A, 2B and 2C  $\epsilon_{FRET} = 0.23, 0.29$  and  $0.276$  respectively. Hence, the calculated distances ( $R_{DA}$ ) of F-W<sub>3</sub>T compound are  $\sim 36.07\text{\AA}$  (from colchicine binding site),  $\sim 57\text{\AA}$  (from ANS binding site) and  $\sim 65\text{\AA}$  (from Taxol binding site) in tubulin.

**Fluorescence measurement of tubulin-DCVJ complex after incorporation with W<sub>3</sub>T**

For this experiment,  $2\ \mu\text{M}$  of DCVJ was added with  $10\ \mu\text{M}$  of tubulin in BRB80 solution for 1 h. Then, we prepared four aliquots of the incubated solution. After that, we added four different concentration of W<sub>3</sub>T compound into four aliquots solution and the four solutions was incubated for another 10 min at  $37\text{ }^\circ\text{C}$ . Then the emission spectrum was recorded from 450 to 650 nm after exciting the solution at 430 nm at  $37\text{ }^\circ\text{C}$  using Quanta Master Spectrofluorometer (QM-40) equipped with Peltier. We recorded the emission spectrum of DCVJ for control.

**Immunofluorescence Microscopy<sup>10</sup>**

The A549 cells were grown on cover glass bottom dish at a density of 20000 cells per plate. Then the cells were treated overnight with  $1\ \mu\text{M}$  of W<sub>3</sub>T in complete DMEM. Untreated cells grown overnight on glass bottom dish were taken as control. Thereafter the cells were fixed with 4% formaldehyde solution and permeabilized with 0.1% Triton-X-100. Then the fixed cells were washed with PBS and incubated with the respective primary antibodies (anti-alpha Tubulin, anti-Mad2, anti-BubR1, anti-p53 and anti-p21) overnight at  $4^\circ\text{C}$ . After that it was treated with secondary antibody (Goat pab to Rb IgG (Cy3.5 ®); 1:600) for 2h at room temperature and later nuclear staining was performed through incubation with Bisbenzimid H 33258 (hoechst) ( $1\ \mu\text{g}/\text{mL}$ ) for 30 min. Finally, the cells were washed with 1X PBS and observed in the inverted microscope (Olympus IX 83) equipped with an Andor iXon3 897 EMCCD camera in DIC mode, 405 and 561 nm fluorescence channels.

**Cell viability assay**

Cell viability of triazine compounds were evaluated by the reduction of the yellow tetrazolium MTT (3-(4, 5-dimethylthiazolyl-2)-2, 5-diphenyltetrazolium bromide) to the intracellular purple formazan by metabolically active cells through the action of dehydrogenase enzymes, to generate reducing equivalents such as NADH and NADPH. The resulting formazan is solubilized in organic solvents and quantified by spectrophotometry. Briefly, the cells were grown at a density of 10000 cell per well in a 96-well plate for 24 h, then the cells were treated with different concentrations of compounds in complete DMEM. Untreated cells were used as control. After 24 h, MTT solution was added to each well and incubated in  $37^\circ\text{C}$  for 4h. The insoluble formazan obtained was solubilized in DMSO: MeOH (1:1) and the absorbance recorded at 550 nm wavelength in ELISA plate reader (Thermo; Multiskan™ GO Microplate Spectrophotometer). Here, following different cell types (A549, MCF7, HeLa, B16F10, C2C12, MCF10A and WI38)

that have been used for the evaluation of cell viability. Results were expressed as percentage of viability = [(A550 (treated cells)-(background)/ (A550 (untreated cells)-background)] × 100.

### **Apoptosis assay<sup>11</sup>**

A549 cells were seeded at a density of  $\sim 5 \times 10^5$  cells per well in a 6-well plate. Then cells were treated with variable concentrations of W<sub>3</sub>T overnight in complete DMEM. Cells were then trypsinized, collected by centrifugation and stained with 2.5  $\mu$ L of Annexin V and Propidium iodide (PI) per 100  $\mu$ L of assay buffer for 45 min at room temperature. The cells were then diluted with another 400  $\mu$ L of assay buffer per sample and analyzed in BD LSRFORTESA flow cytometer using emission filters at 530 and 610 nm respectively. FACS DIVA software was used for analysis of data.

### **Cell cycle analysis**

A549 cells were plated at a density of  $5 \times 10^5$  cells per well in a 6 well plate. Then, the cells were treated with W<sub>3</sub>T overnight in complete DMEM. Untreated cells were considered as control. After that the cells were trypsinized and centrifuged at 3000 rpm for 3 min to collect the pellet. The entire pellet was fixed in ice cold ethanol and kept at 4°C overnight. Then, we added propidium iodide and RNase A to the cell suspension in PBS and kept for 45 min at RT. Suspension of cells were homogenated and transferred into FACS tube and analysed by BD LSRFORTESA flow cytometer. Finally, the recorded data was analyzed using FACS DIVA software.

### **Cell Cycle Analysis through cell synchronization**

A549 cells plated at a confluency of  $5 \times 10^5$  in 6 well plates were treated with and without nocodazole for 24 h. Nocodazole was washed using fresh DMEM media. The cells were incubated without or with W<sub>3</sub>T for 4 and 6 h. Then release of the mitotic block was examined in a BD LSRFORTESA flow cytometer and analyzed using FACS DIVA software.

### **Effect of W<sub>3</sub>T on Mitochondrial Membrane Potential<sup>12</sup>**

A549 cells were cultured in six-well plates and treated with W<sub>3</sub>T overnight. Subsequently, cells were suspended and intracellular mitochondrial membrane potential ( $\Delta\psi_m$ ) was evaluated using BD MitoScreen according to the manufacturer's instructions. Briefly, the suspended cells were washed thoroughly and working concentrations of JC1 dye in 1X assay buffer was added. JC-1 (5,5',6,6'-tetrachloro-1,1',3,3'- tetraethylbenzimidazolcarbocyanine iodide) is a lipophilic fluorochrome that is used to evaluate the status of the  $\Delta\psi$ . Then it was incubated for 15 min at 37 °C in CO<sub>2</sub> incubator. Finally, the cells were washed with 1X assay buffer and evaluated through FACS (LSRFORTESA) at 527 nm and 590 nm.

### **Western Blot Analysis**

In 6-well plate, cells were seeded at a density of  $\sim 5 \times 10^5$  /well. Cells were then treated with T-3W for 24 h. Cells were lysed and protein isolation was carried out in RIPA buffer. Then concentration of the protein was determined using Bradford assay. After heating at 90 °C for 10 min, proteins were subjected to SDS-PAGE and transferred electrophoretically to PVDF membrane. Then membranes were blocked with skimmed milk and incubated overnight with their respective primary antibodies (anti-cleaved caspase 3, anti-p53, anti-p21, anti-Cytochrome

c and anti- $\alpha$ -tubulin) at 4<sup>0</sup>C temperature. Subsequently the membranes were incubated with anti-mouse/anti-rabbit peroxidase-conjugated secondary antibodies (1:5000) for 1 h at room temperature. Immunoreactivity was developed by an enhanced chemiluminescence detection system using HRP substrate (Luminata Forte Western HRP substrate, Merck Millipore, Darmstadt, Germany). Finally, the protein band intensity was normalized with the loading control and the relative expression was quantified.

### **Growth inhibition of multicellular tumor 3D spheroids**

A parental monolayer of A549 cells were grown and transferred to 35 mm cell culture dishes, previously coated with 1% agarose and incubated in 37<sup>0</sup>C till the formation of 3D spheroids. Then the spheroids were treated with W<sub>3</sub>T. In a separate control no treatment was given. Then, the morphological changes of 3D spheroid were investigated up to 9 days from the day of the treatment by inverted Olympus microscope equipped with EMCCD camera. Volume of the spheroid were calculated using the formula mentioned below  $V = 0.5 \times \text{Length} \times \text{Width}^2$

### ***In vivo* study**

We have determined the acute maximum tolerated dose (MTD) following single i.p. administration to six groups of different dose levels of W<sub>3</sub>T (20, 40, 80, 120, 140 and 160 mg/kg) comprising of three healthy C57BL/6J female mice in each group. The dose just below the dose level that killed at least one mice in treatment group after a maximum of 28 days was considered as MTD dose. Herein, we have observed that the dose just above the MTD dose showed some adverse effect like reduced motor activity and shivering with loose stool excretion and subsequent weight loss in the animals followed by the death of one mice in that particular dose group. Animals were kept in pathogen-free laboratory throughout the experiments. All animal experiments have been approved and were performed in compliance with the relevant laws of the institutional animal ethics committee (IAEC) of CSIR-Indian Institute of Chemical Biology, India.

*In vivo* studies were performed on C57BL/6J female melanoma mice model. Animals were housed in pathogen-free environment in our institute's animal house. Tumors were generated by one-time subcutaneous injection of B16F10 cells ( $\sim 2 \times 10^6$  cells/animal) in PBS. Tumor growth was measured by slide calipers and the volume of the tumor was calculated using the formula  $V = 0.5 \times \text{length} \times \text{width}^2$ . After the generation tumor, mice were divided in three groups having five mice in each group (group 1, group 2 and group 3). Then each mice of the group1 was treated with W<sub>3</sub>T (1mg/kg bodyweight), group 2 was treated with colchicine (1mg/ kg bodyweight) and group 3 was treated with only PBS considered as control, which was treated with sterile saline. First day of the treatment was considered as 0 day and it continued up to 14 days and simultaneously we recorded the tumor volume as well as body weight of the mice from 0 to 14 days. After 14 days, the mice were sacrificed by cervical dislocation. Volume of the tumors was measured. For the fixation of the tumors, we have used 4% formalin in PBS, embedded in paraffin, and partitioned with a thickness of 4  $\mu$ m using Leica Rotary Microtome. For histological study, the slices were stained with hematoxylin and eosin (HE). Then, the stained slices were imaged by microscope under 10X objective in bright field.

### **STD NMR sample preparation and experiments**

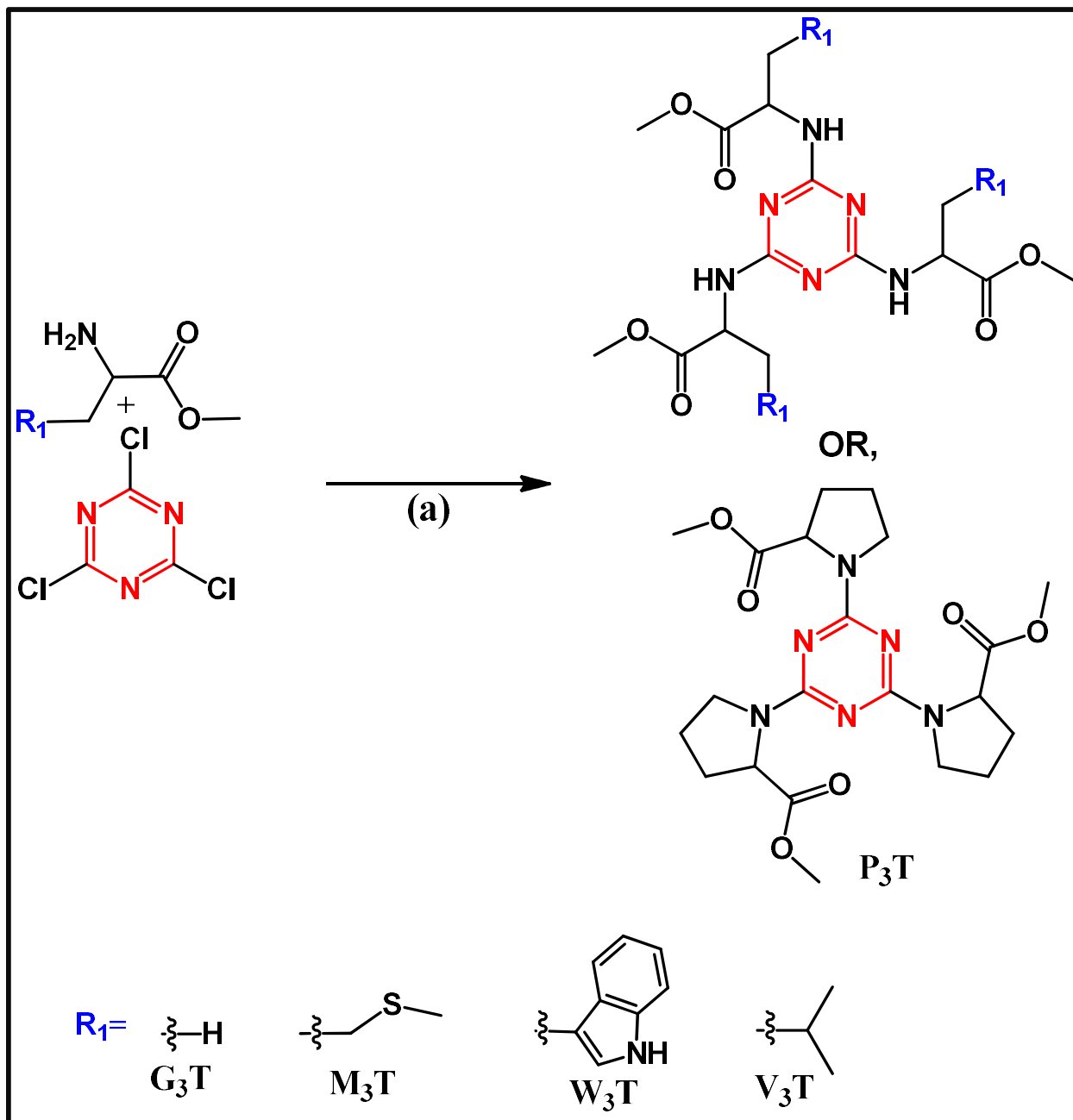
'Epitopes' are the protons those are closer to the protein during interactions. The epitopes are identified using the STD-NMR study. The NMR samples of the ligands bound to nonpolymerized tubulin  $\alpha/\beta$ -heterodimers were prepared using a 300  $\mu$ M concentration of the W<sub>3</sub>T compound and 10  $\mu$ M of tubulin in D<sub>2</sub>O, 10 mM NaPi, 0.1 mM GTP. We used minimum amount of D6-DMSO to solubilize the W<sub>3</sub>T. We recorded the NMR by Bruker AVANCE 600 MHz spectrometer equipped with a triple-channel cryoprobe with saturation time 2s. STD effects were calculated using the equation  $ASTD = (I_0 - I_{sat})/I_0 = I_{STD}/I_0$  where intensity of the signals in the STD NMR spectrum (ISTD) with signal intensities of a reference spectrum ( $I_0$ ). The highest STD signal considered as 100% STD effect and other STD signals were calculated accordingly.

**TR-NOESY experiments** with non-polymerized tubulin  $\alpha/\beta$ -heterodimers were performed with mixing times of 200 ms. Strong negative NOE cross peaks were observed compare to the Free State, indicating there is interaction ligand with the receptor (tubulin). All the data were calculated using Mnova software.

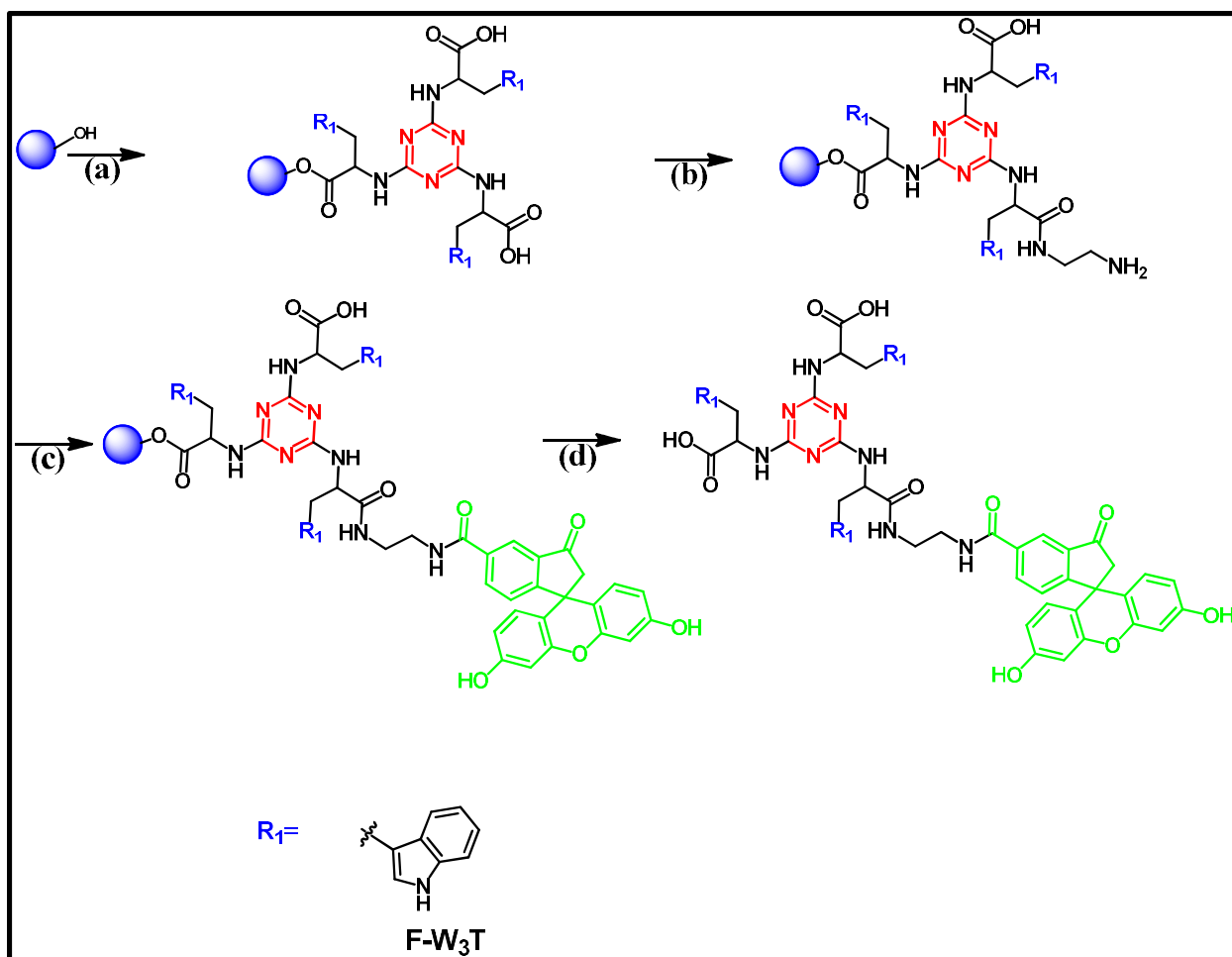
## References

1. A. Hyman, D. Drechsel, D. Kellogg, S. Salser, K. Sawin, P. Steffen, L. Wordeman, T. Mitchison, *Methods Enzymol* 1991, **196**, 478.
2. A. D. Becke, *J. Chem. Phys.* 1993, **98**, 5648.
3. C. Lee, W. Yang, R. G. Parr, *Phys. Rev. B* 1988, **37**, 785.
4. D. Andrae, U. Haeussermann, M. Dolg, H. Stoll, H. Preuss, *Theor. Chim. Acta* 1990, **77**, 123.
5. Gaussian 09, Revision D.01, M. J. Frisch et al Gaussian, Inc., Wallingford CT, 2013.
6. J. Kong, C. A. White, A. I. Krylov, D. Sherrill, R. D. Adamson, T. R. Furlani, M. S. Lee, A. M. Lee, S. R. Gwaltney, T. R. Adams, C. Ochsenfeld, A. T. B. Gilbert, G. S. Kedziora, V. A. Rassolov, D. R. Maurice, N. Nair, Y. Shao, N. A. Besley, P. E. Maslen, J. P. Dombroski, H. Daschel, W. Zhang, P. P. Korambath, J. Baker, E. F. C. Byrd, T. Van Voorhis, M. Oumi, S. Hirata, C.P. Hsu, N. Ishikawa, J. Florian, A. Warshel, B. G. Johnson, P. M. W. Gill, M. Head-Gordon, J. A. Pople, *J. Comput. Chem.* 2000, **21**, 1532.
7. O. Trott, A. J. Olson, *J. Comput. Chem.* 2010, **31**, 455.
8. B. Gigant, C. Wang, R.B. Ravelli, F. Roussi, M.O. Steinmetz, P.A. Curmi, A. Sobel, M. Knossow, *Nature* 2005, **435**, 519.
9. P. Mondal, G. Das, J. Khan, K. Pradhan, S. Ghosh, *ACS Chem. Neurosci.* 2018, **9**, 615.
10. A. Saha, S. Mohapatra, P. Kurkute, B. Jana, P. Mondal, D. Bhunia, S. Ghosh, S. Ghosh, *Chem. Commun.* 2015, **51**, 2249.
11. A. Saha, S. Mohapatra, G. Das, B. Jana, S. Ghosh, D. Bhunia, S. Ghosh, *ACS Appl. Mater. Interfaces* 2017, **9**, 176.
12. J. Friedrich, C. Seidel, R. Ebner, L. A. Kunz-Schughart, *Nature Protocols.* 2009, **4**, 309.

Electronic Supplementary Schemes and Figure

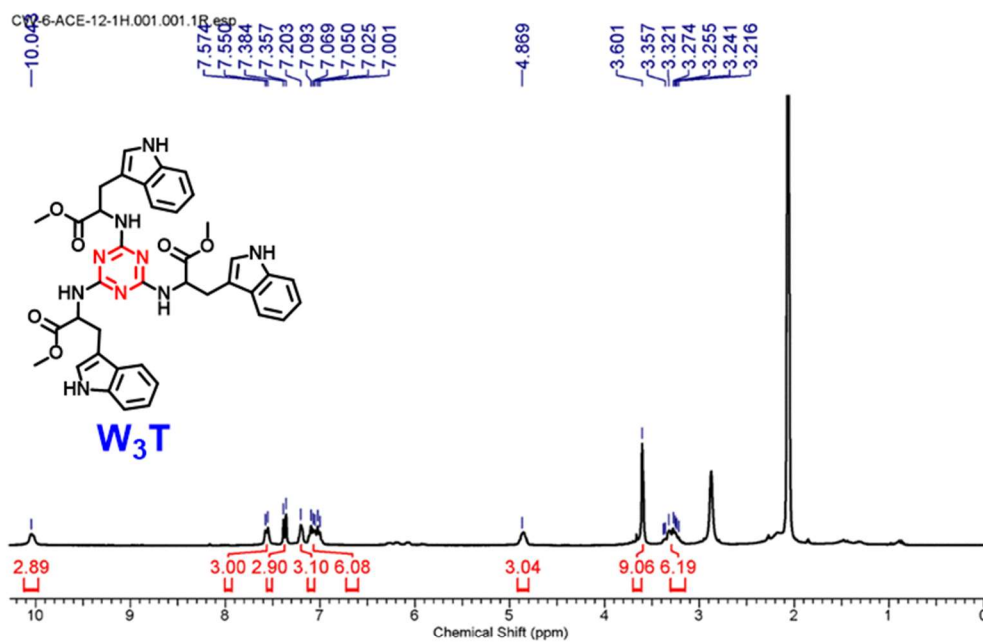


**Scheme Sc1.** Synthetic scheme for triazine derivatives. Reaction conditions: (a) DIPEA, dry THF in inert condition for overnight.



**Scheme Sc2.** Synthesis scheme for fluorescein tagged aryl substituted triazine derivatives. **Reaction conditions:** (a) W<sub>3</sub>T-COOH, HBTU and DIPEA. (b) Ethylene diamine, HBTU and DIPEA. (c) 5(6)-Carboxyfluorescein, HBTU and DIPEA. (d) TFA.

(A)



(B)

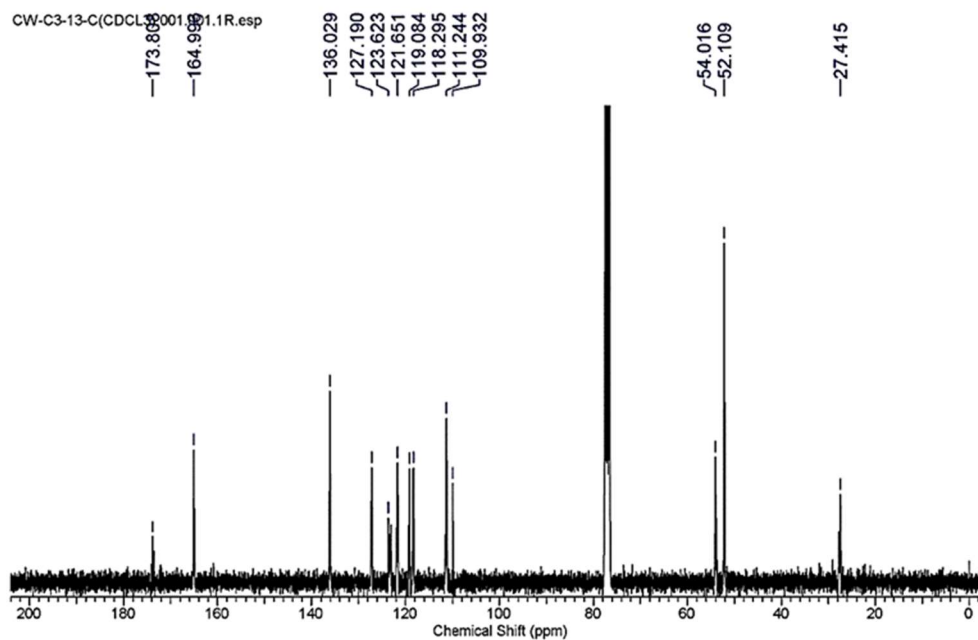


**Figure S1.** (A)  $^1\text{H}$  NMR of **W<sub>3</sub>T** (300 MHz, Acetone- $d_6$ ) and (B)  $^{13}\text{C}$  NMR of **W<sub>3</sub>T** (75 MHz, Chloroform).

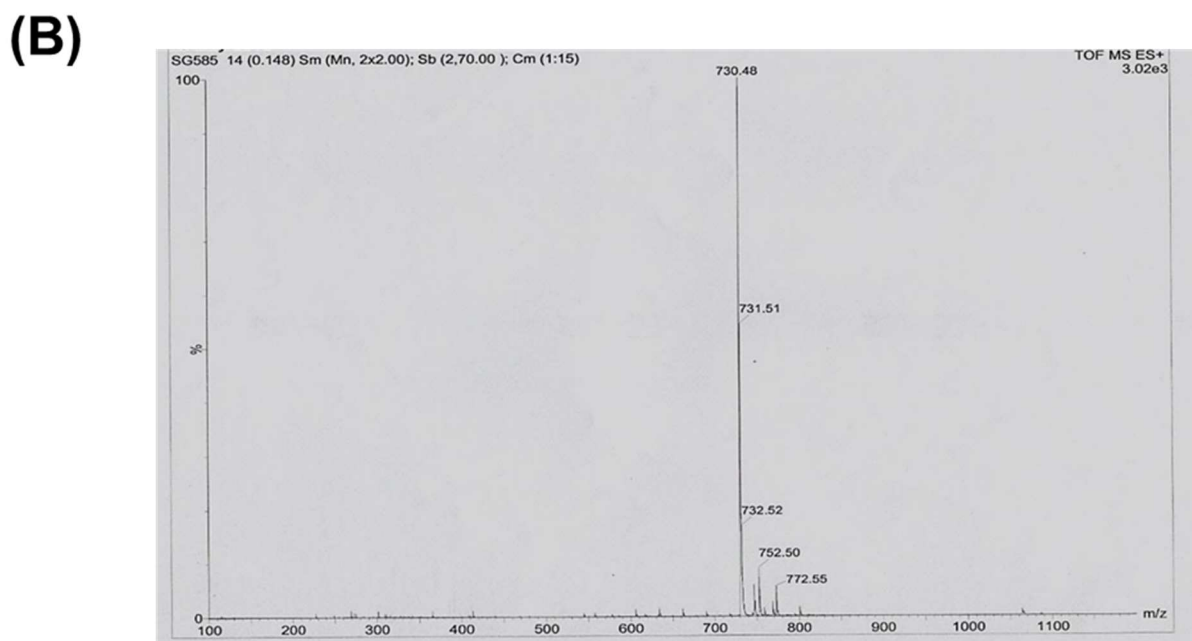
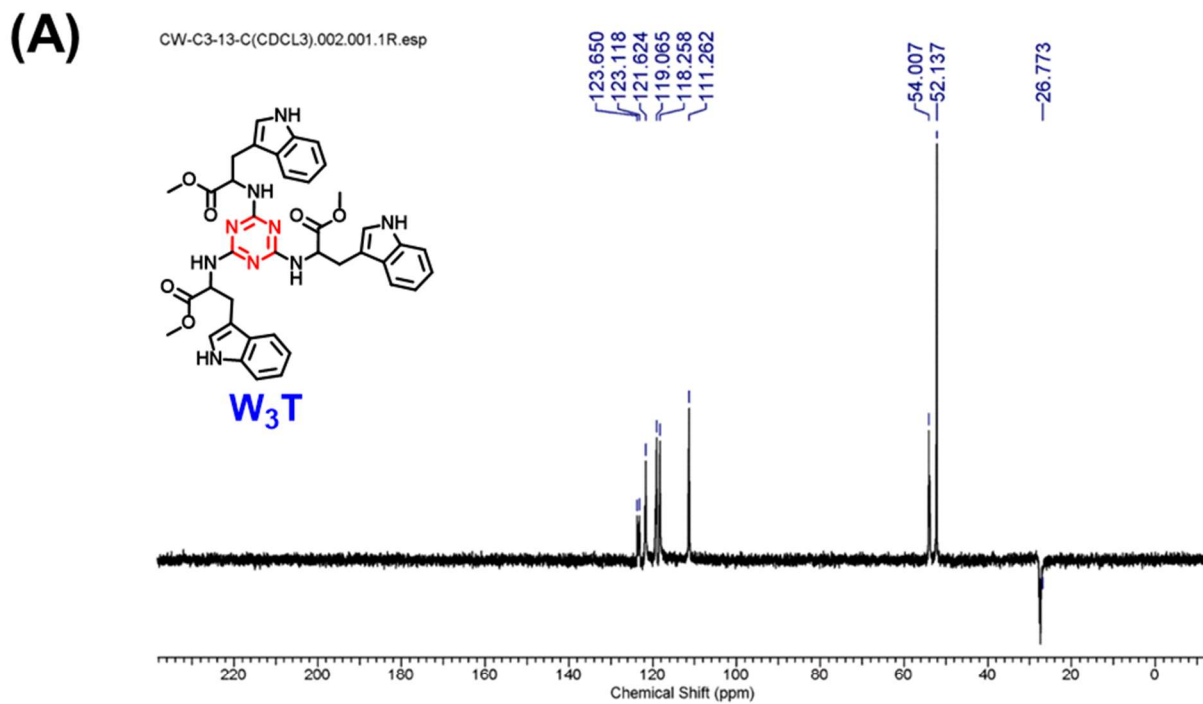
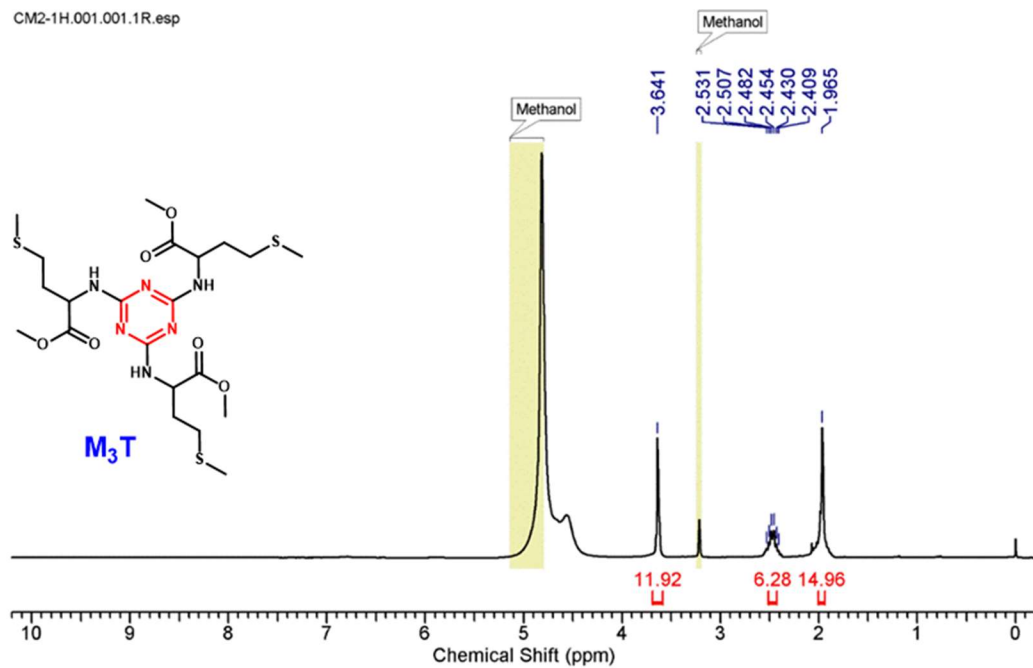


**Figure S2.** (A)  $^{13}\text{C}$ -NMR DEPT-135 of **W<sub>3</sub>T** (150 MHz,  $\text{CDCl}_3$ -d) and (B) ESI Mass spectrum of **W<sub>3</sub>T**.

(A)



(B)

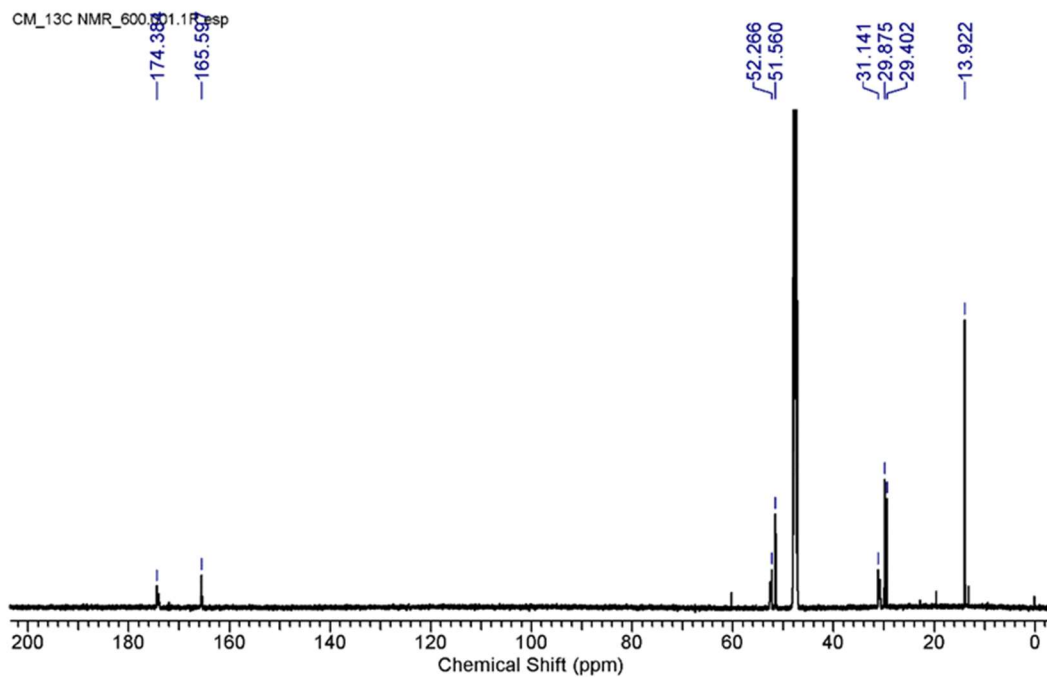
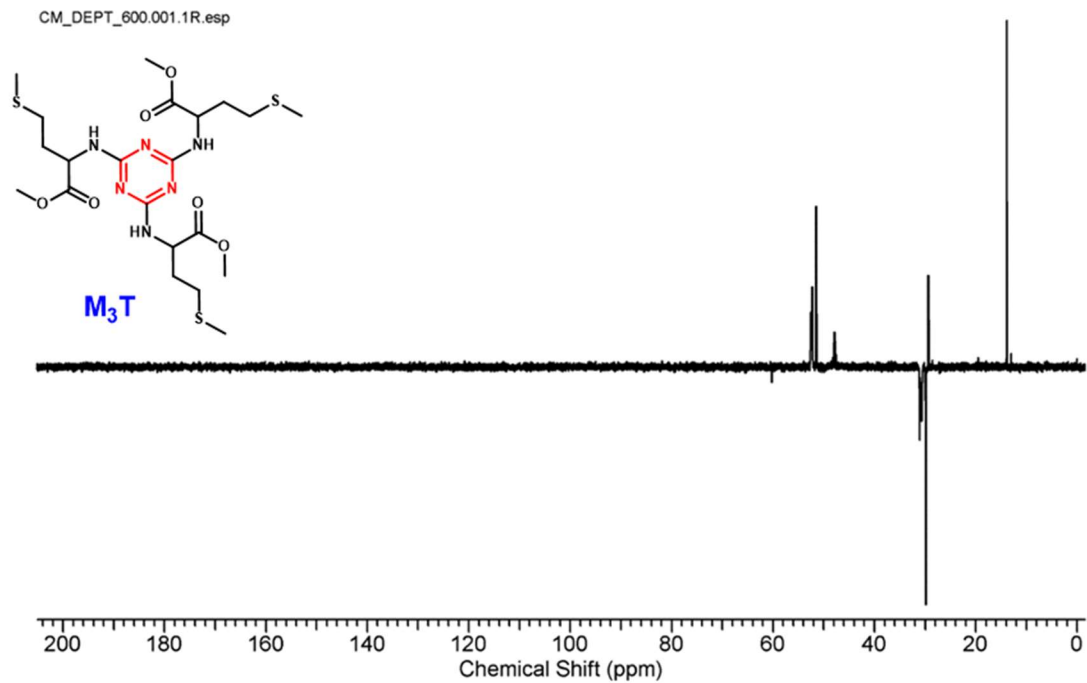


**Figure S3.** (A)  $^1\text{H}$  NMR of **M<sub>3</sub>T** (300 MHz, METHANOL- $\text{d}_4$ ). (B)  $^{13}\text{C}$  NMR of **M<sub>3</sub>T** (150 MHz, METHANOL- $\text{d}_4$ ).

(A)



(B)

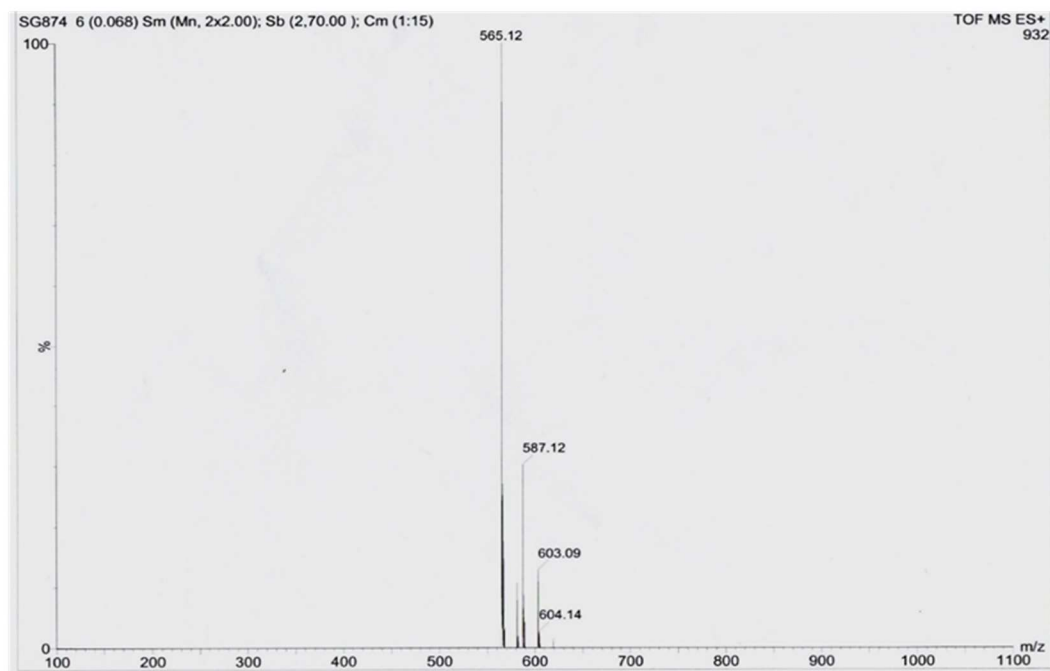


**Figure S4.** (A)  $^{13}\text{C}$ -NMR DEPT-135 of **M<sub>3</sub>T** (150 MHz, METHANOL- $d_4$ ) and (B) ESI Mass spectrum of **M<sub>3</sub>T**.

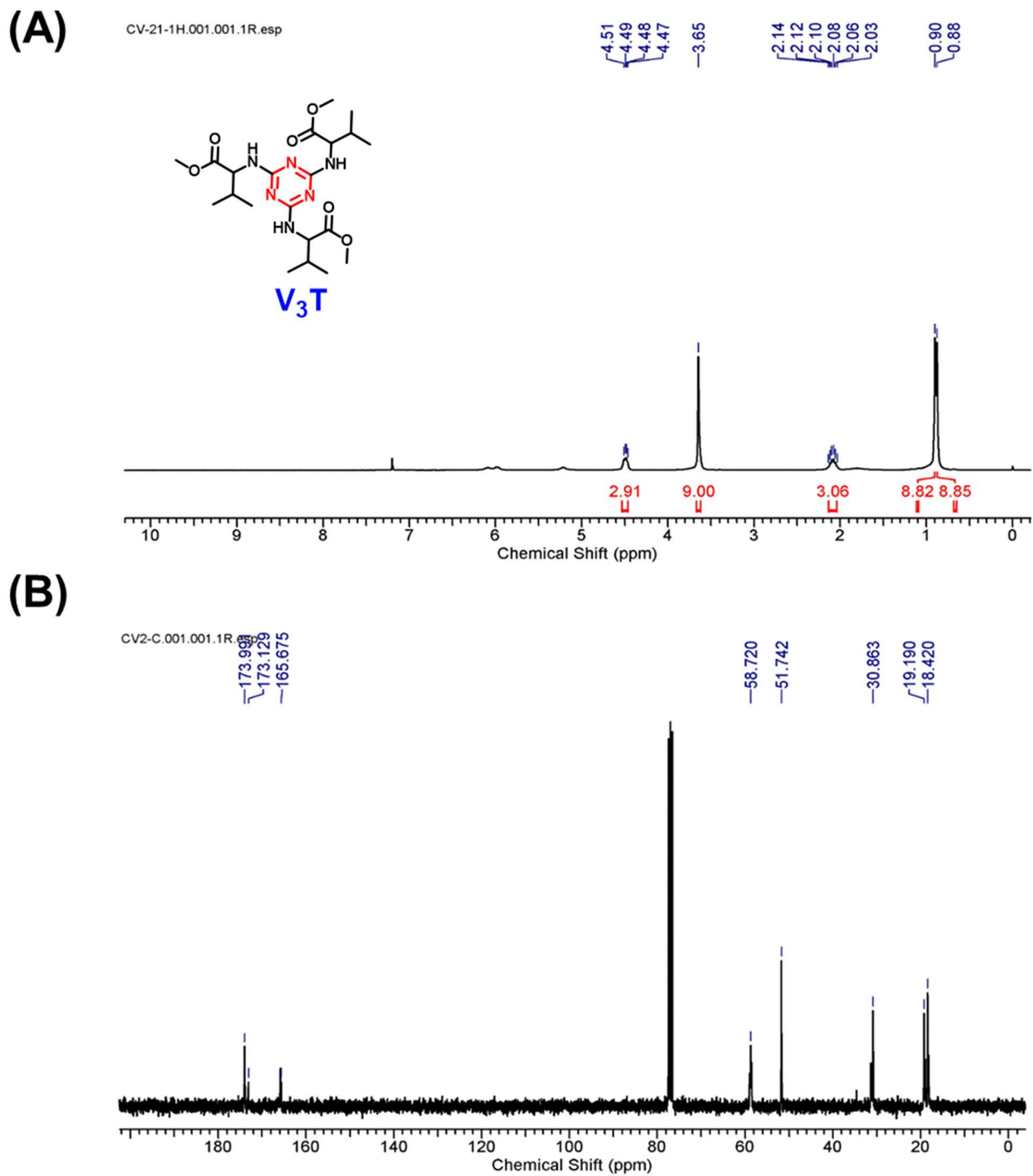


**Figure S5.** (A)  $^1\text{H}$  NMR of  $\text{V}_3\text{T}$  (300 MHz,  $\text{CDCl}_3$ ). (B)  $^{13}\text{C}$  NMR of  $\text{V}_3\text{T}$  (75 MHz,  $\text{CDCl}_3$ ).

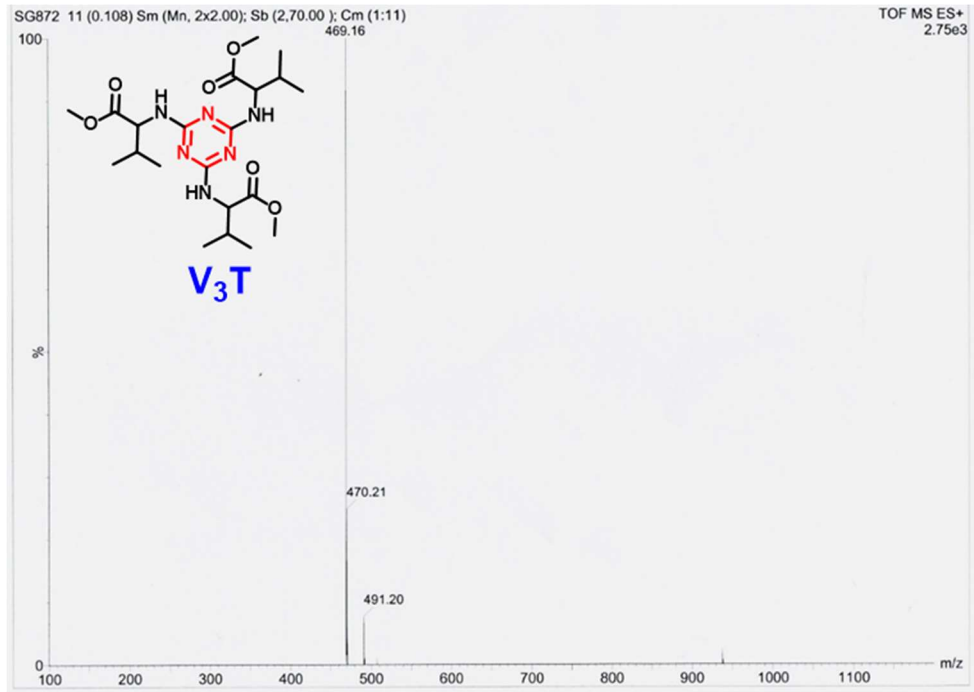
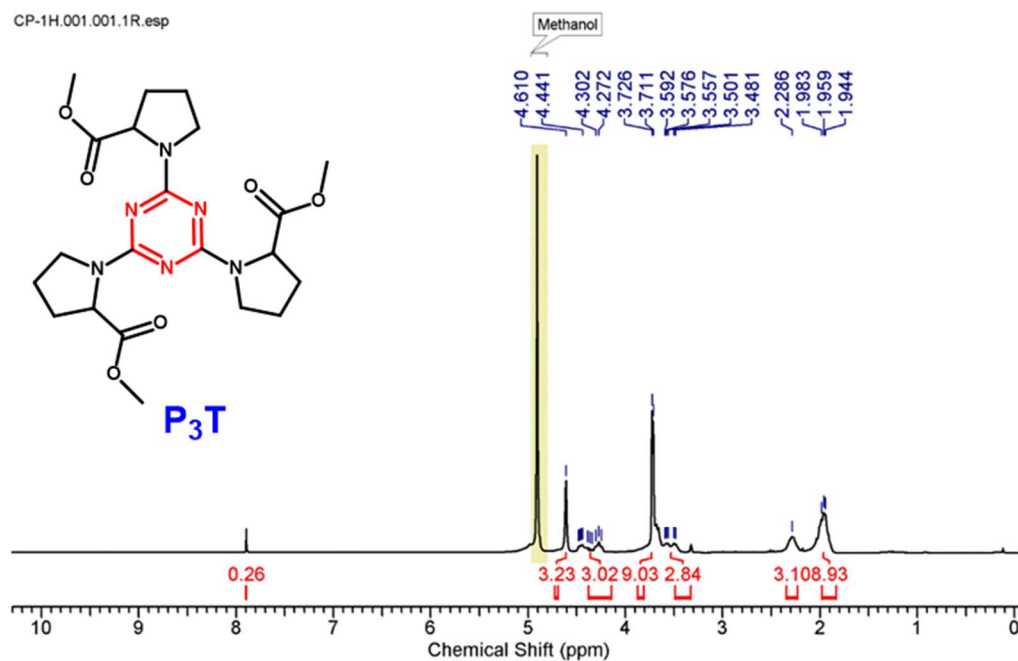


**Figure S6.** ESI Mass spectrum of **V<sub>3</sub>T**.

(A)



(B)

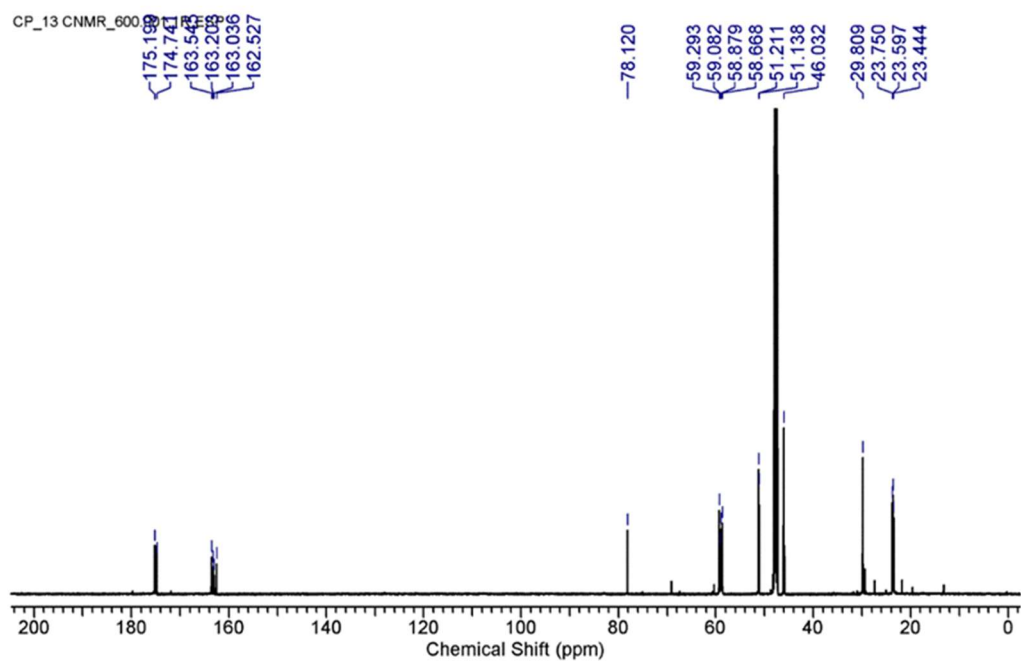
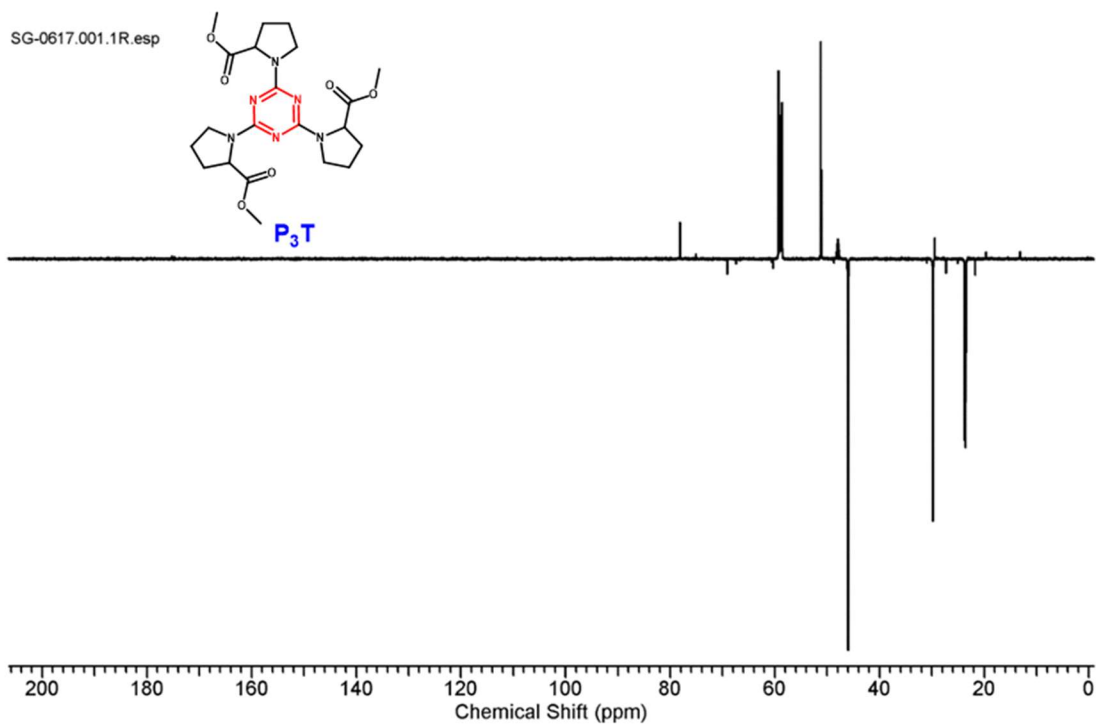


**Figure S7.** (A)  $^1\text{H}$  NMR of **P<sub>3</sub>T** (300 MHz, METHANOL- $\text{d}_4$ ). (B)  $^{13}\text{C}$  NMR of **P<sub>3</sub>T** (150 MHz, METHANOL- $\text{d}_4$ ).

(A)



(B)

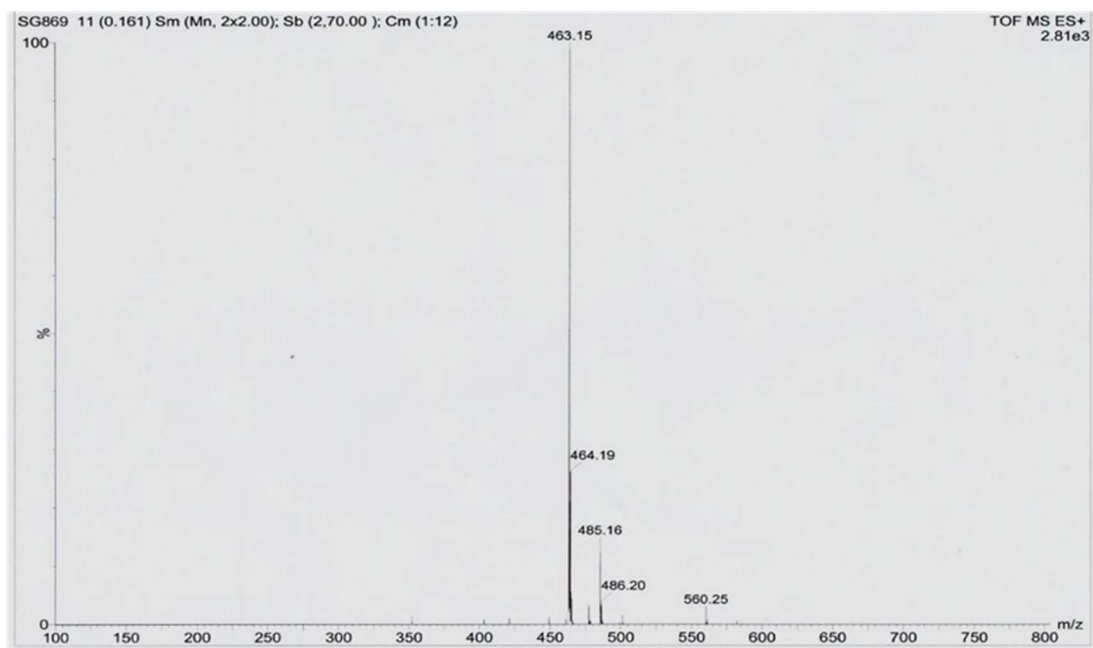
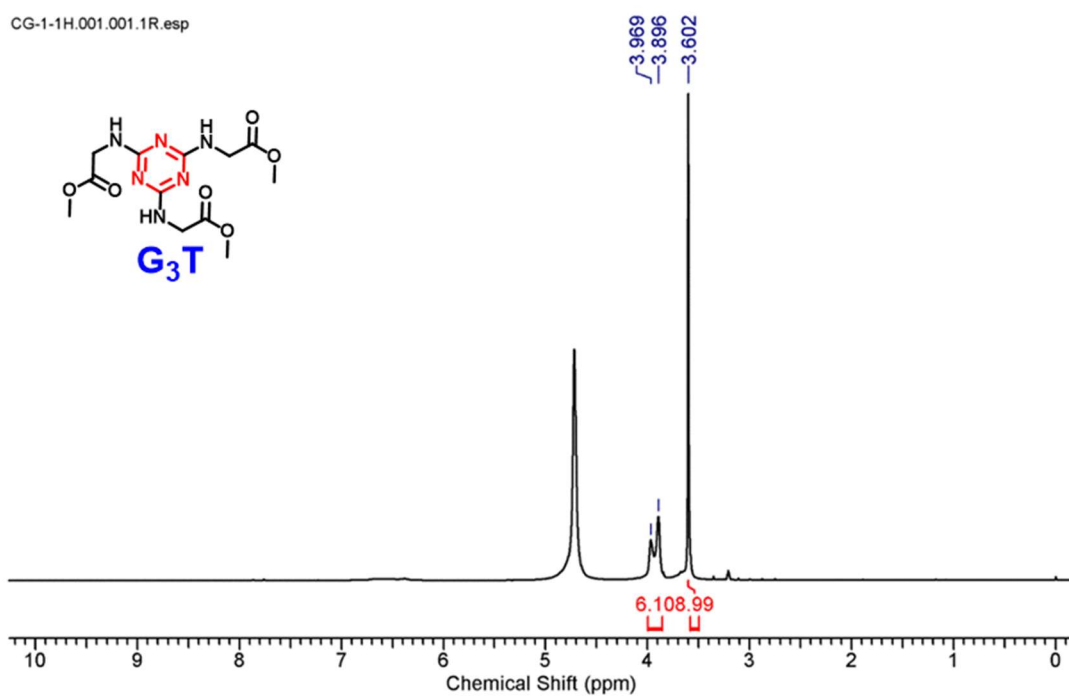


**Figure S8.** (A)  $^{13}\text{C}$ -NMR DEPT-135 of **P<sub>3</sub>T** (150 MHz, METHANOL- $d_4$ ) and (B) ESI Mass spectrum of **P<sub>3</sub>T**.

(A)

CG-1-1H.001.001.1R.esp



(B)

CG-1\_CNMR(600).001.001.1R.esp

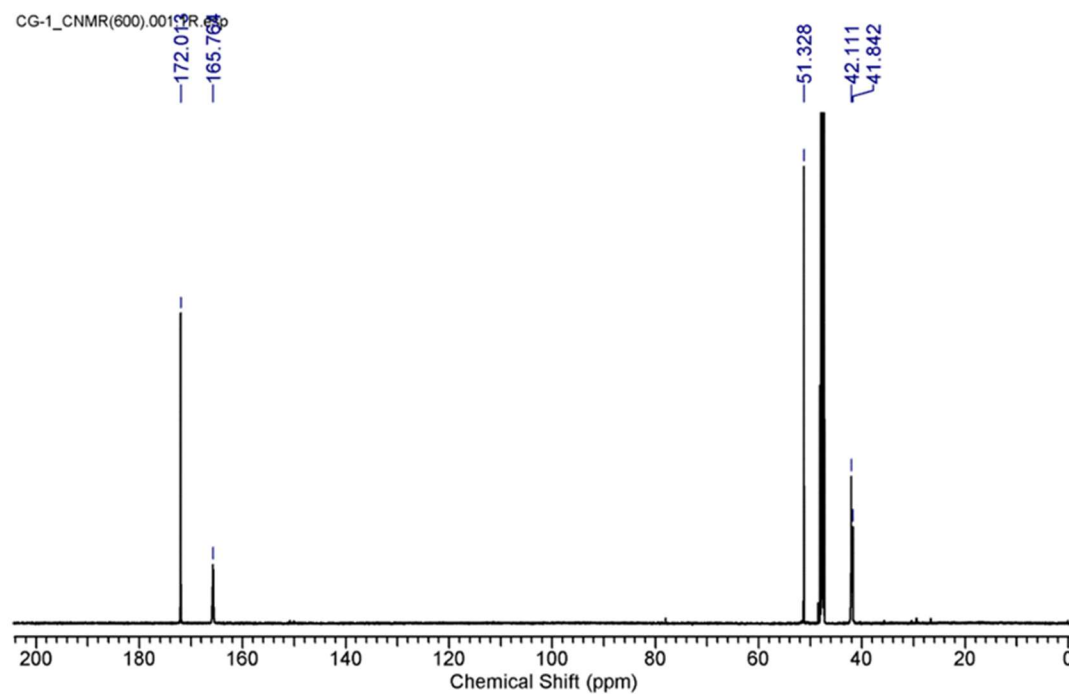


**Figure S9.** (A)  $^1\text{H}$  NMR of **G<sub>3</sub>T** (300 MHz, METHANOL- $\text{d}_4$ ). (B)  $^{13}\text{C}$  NMR of **G<sub>3</sub>T** (75 MHz, METHANOL- $\text{d}_4$ ).

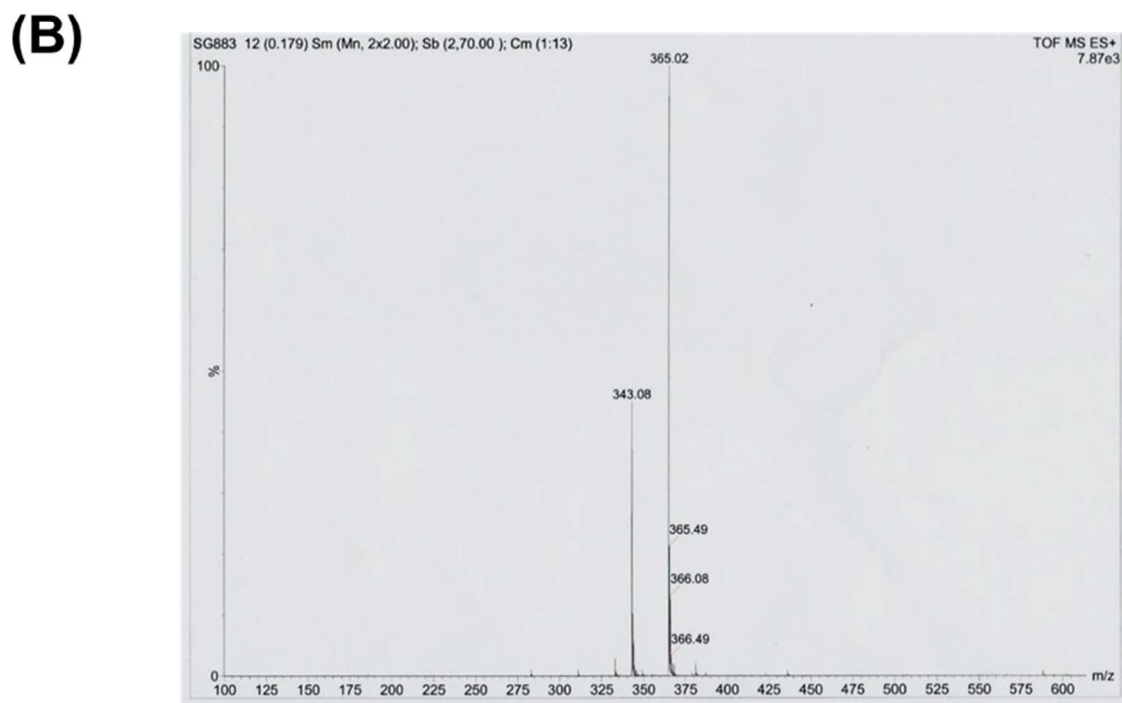
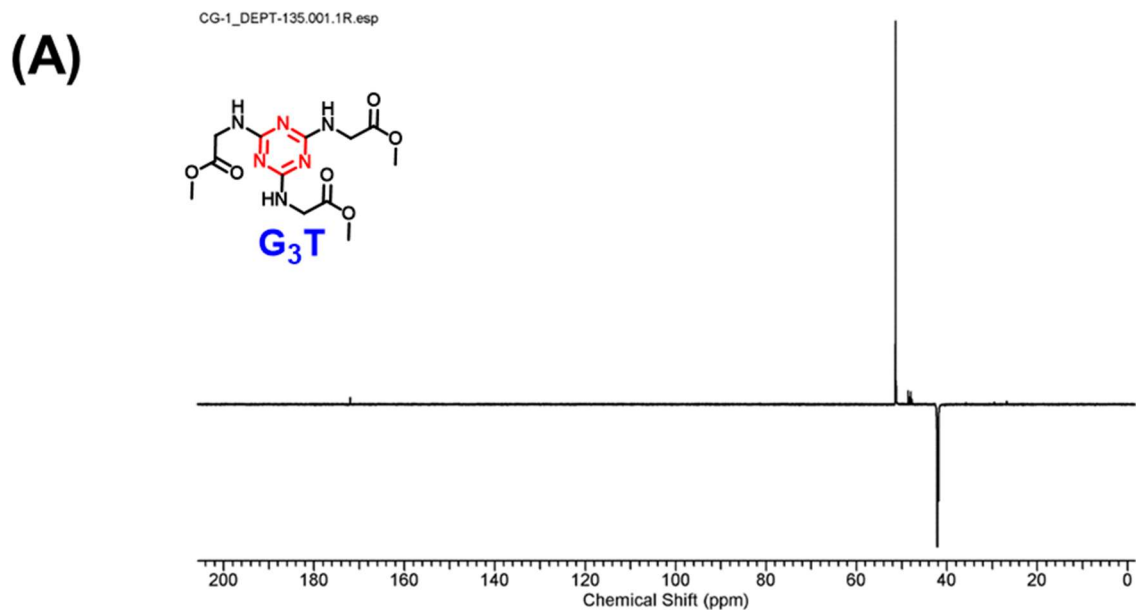
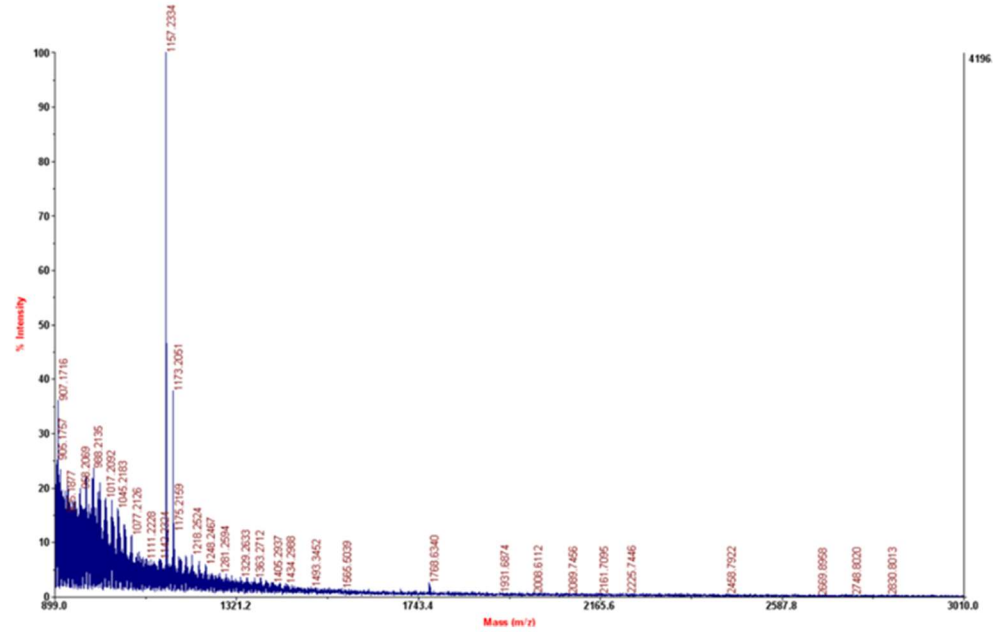
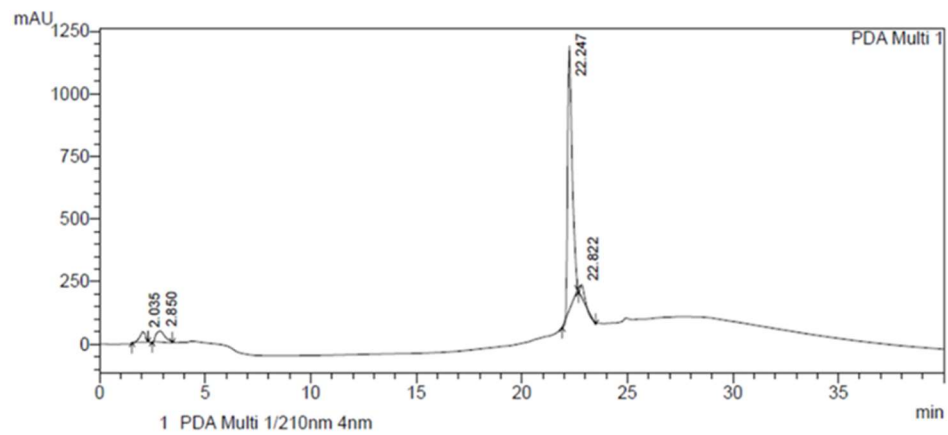


**Figure S10.** (A)  $^{13}\text{C}$ -NMR DEPT-135 of **G<sub>3</sub>T** (75 MHz, METHANOL- $\text{d}_4$ ) and (B) ESI Mass spectrum of **G<sub>3</sub>T**.

(A)



(B)



PeakTable

Peak#	Ret. Time	Area	Height	Area %	Height %
1	2.035	730638	41958	4.002	3.525
2	2.850	1278032	44006	7.000	3.697
3	22.247	15705047	1054638	86.024	88.607
4	22.822	542906	49636	2.974	4.170
Total		18256623	1190238	100.000	100.000

Figure S11. (A) MALDI-Mass spectrum of F-W<sub>3</sub>T and (B) HPLC chromatogram of F-W<sub>3</sub>T.

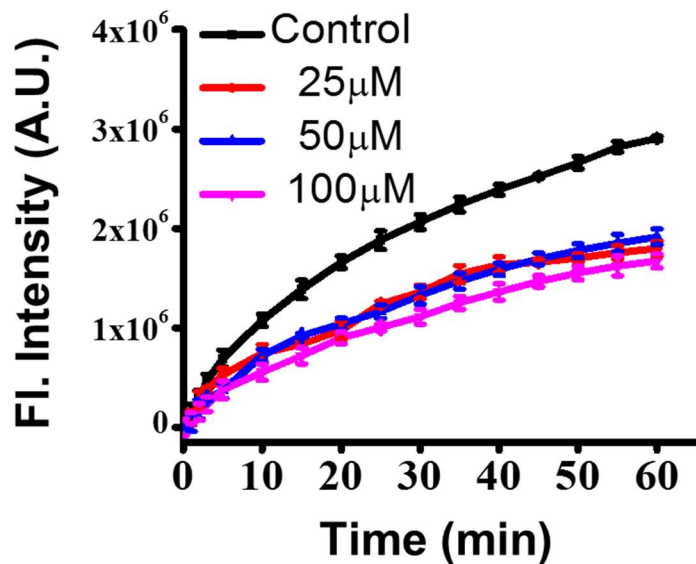


**Figure S12.** Microtubule polymerization assay using DAPI and tubulin upon addition of various concentrations of W<sub>3</sub>T.

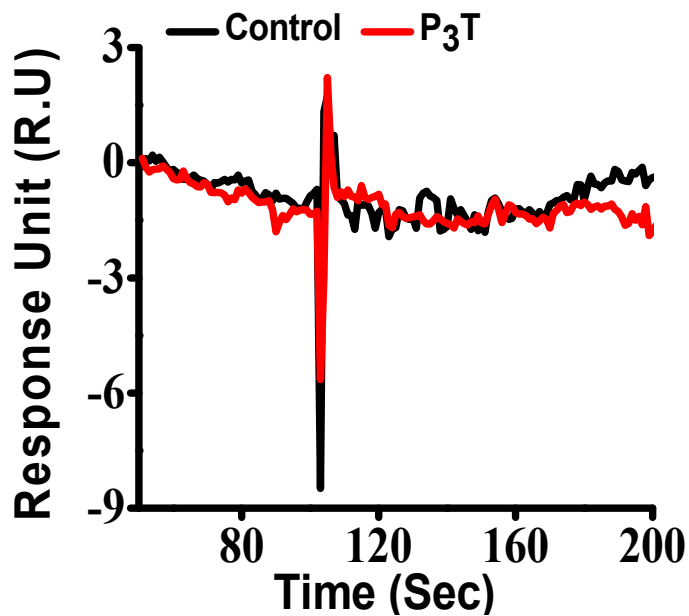


**Figure S13.** SPR sensogram for the kinetic analysis of P<sub>3</sub>T with tubulin.

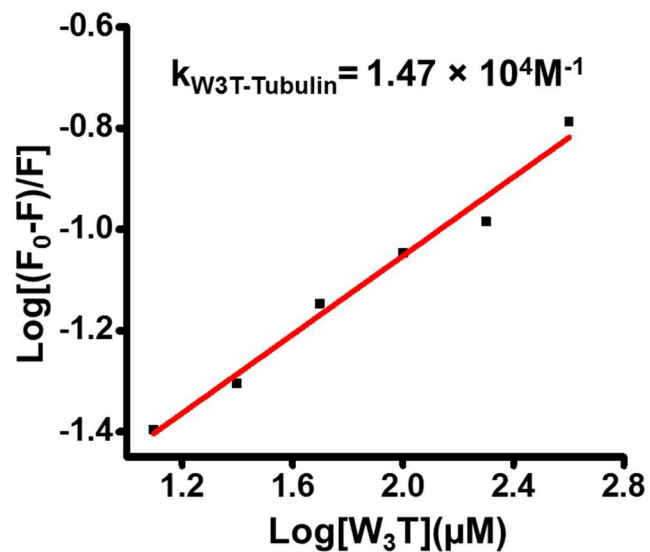


**Figure S14.** Quenching of Tryptophan fluorescence of tubulin in presence of different concentrations of W<sub>3</sub>T to determine binding constant.

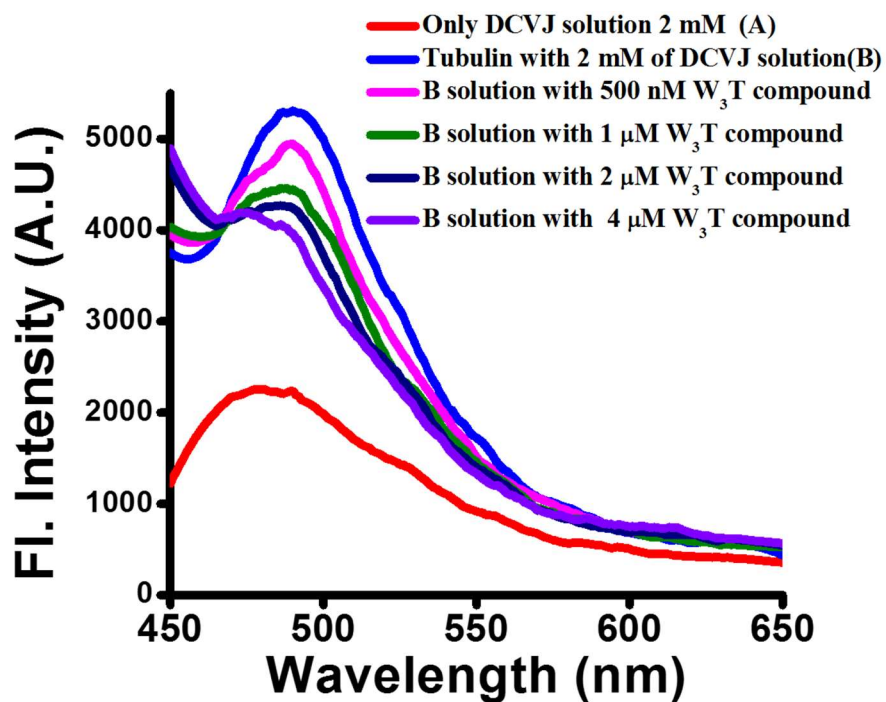


**Figure S15.** Competitive binding study of W<sub>3</sub>T with Tubulin-DCVJ complex.

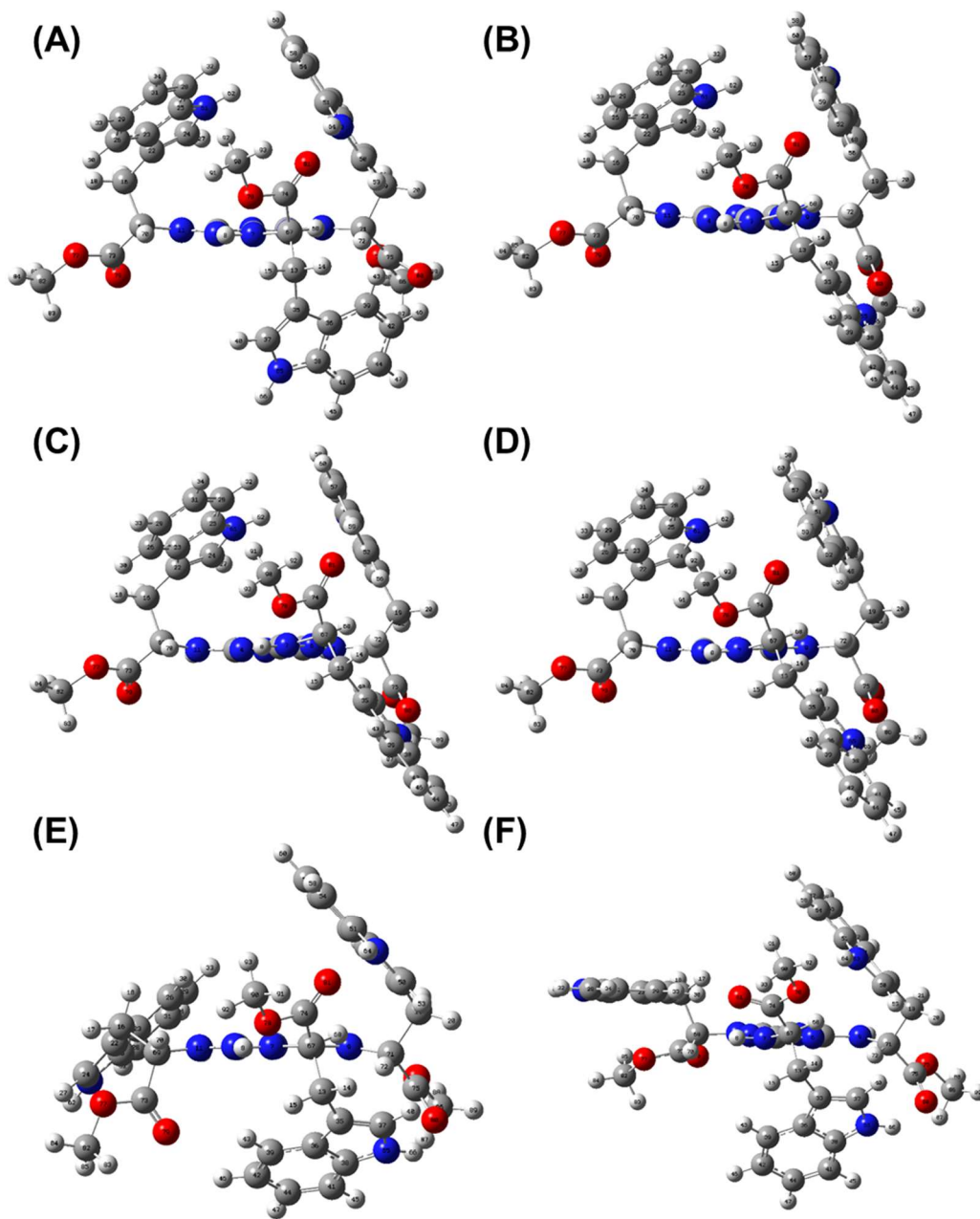


**Figure S16:** Different conformers of **W<sub>3</sub>T** obtained after the semi-empirical calculation, arranged in ascending order (1<sup>st</sup>-6<sup>th</sup>). Corresponding energies (kJ/mol): (A) -6367689.41 (B) -6367689.40 (C) -636782.47 (D) -6367681.73 (E) -6367680.65 (F) -6367680.64.

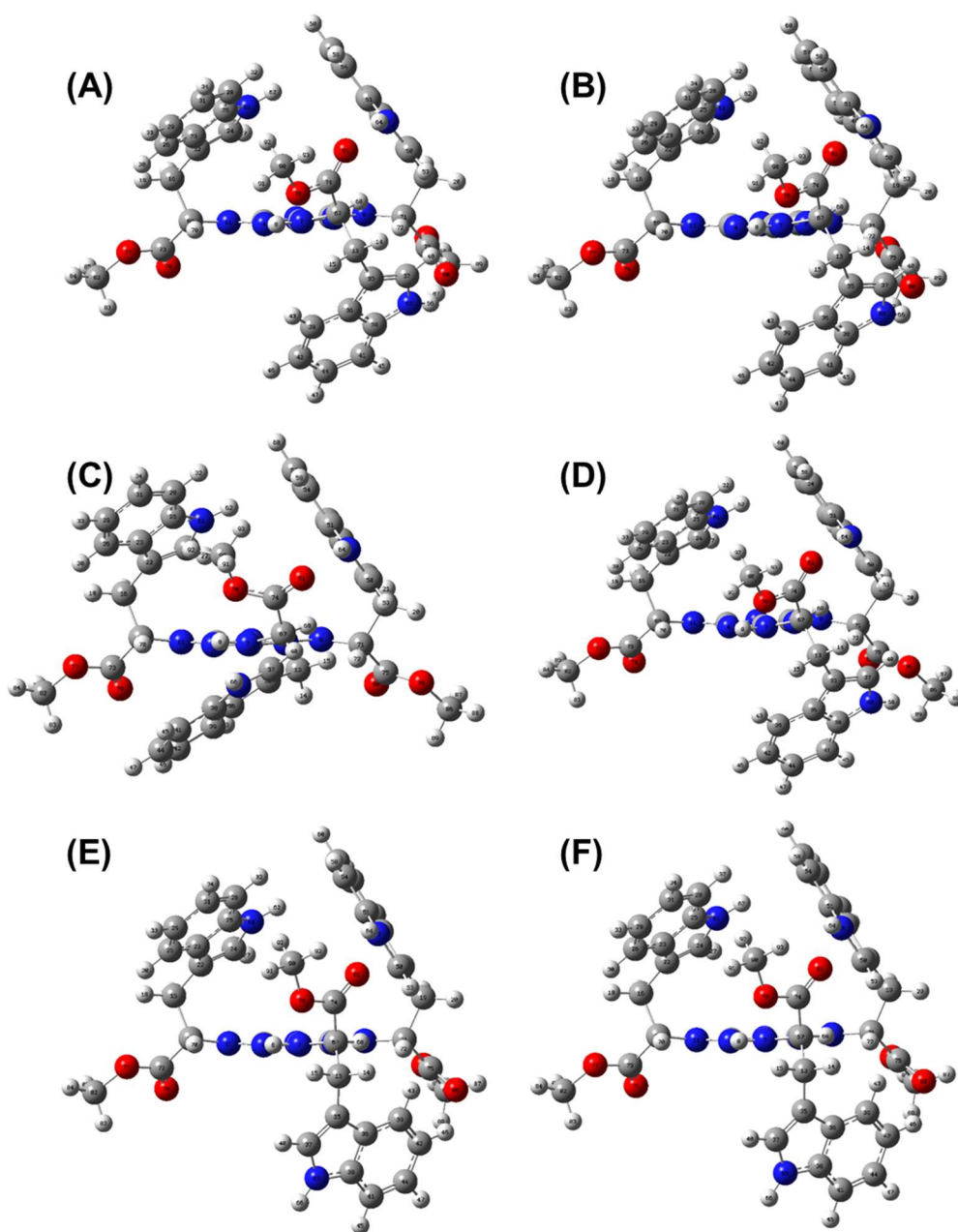


**Figure S17:** Different conformers of **W<sub>3</sub>T** obtained after the semi-empirical calculation, arranged in ascending order (7<sup>th</sup>-12<sup>th</sup>). Corresponding energies (kj/mol): (A) -6367680.28 (B) -6367680.25 (C) -6367680.25 (D) -6367680.24 (E) -6367678.75 (F) -6367677.17.

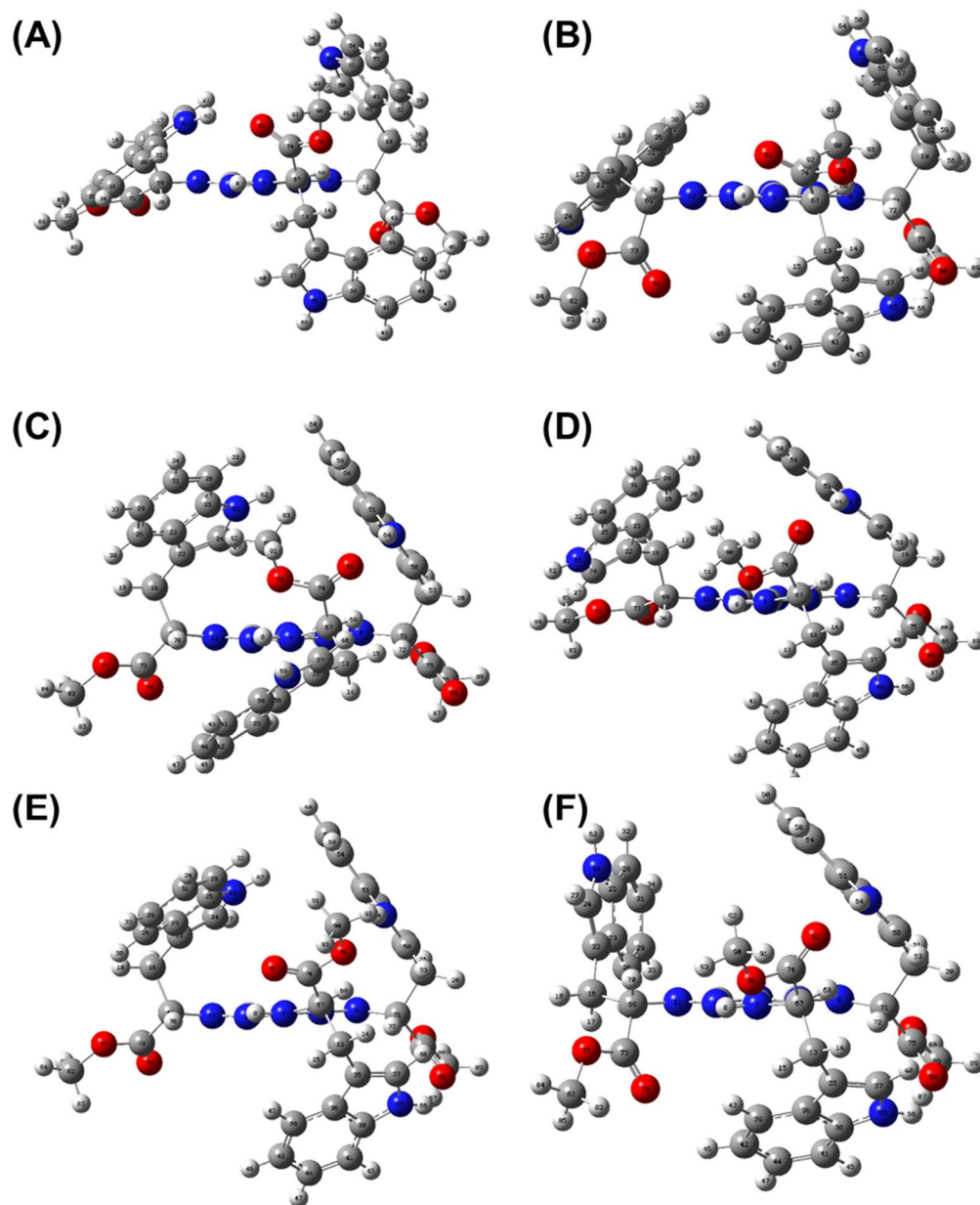


**Figure S18:** Different conformers of  $W_3T$  obtained after the semi-empirical calculation, arranged in ascending order (13<sup>th</sup>-18<sup>th</sup>). Corresponding energies (kJ/mol): (A) -6367676.76 (B) -6367676.61 (C) -6367676.39 (D) -6367675.18 (E) -6367673.12 (F) -6367667.44

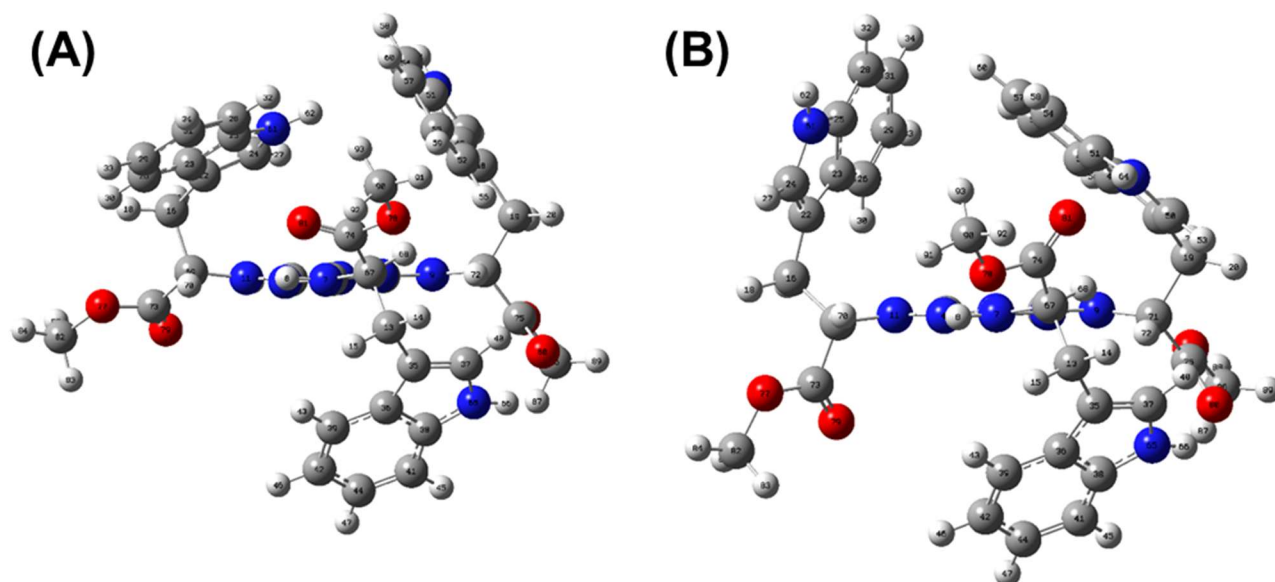


**Figure S19:** Different conformers of **W<sub>3</sub>T** obtained after the semi-empirical calculation, arranged in ascending order (19<sup>th</sup>-20<sup>th</sup>). Corresponding energies (kj/mol): (A) 6367665.94 (B) - 6367665.69.

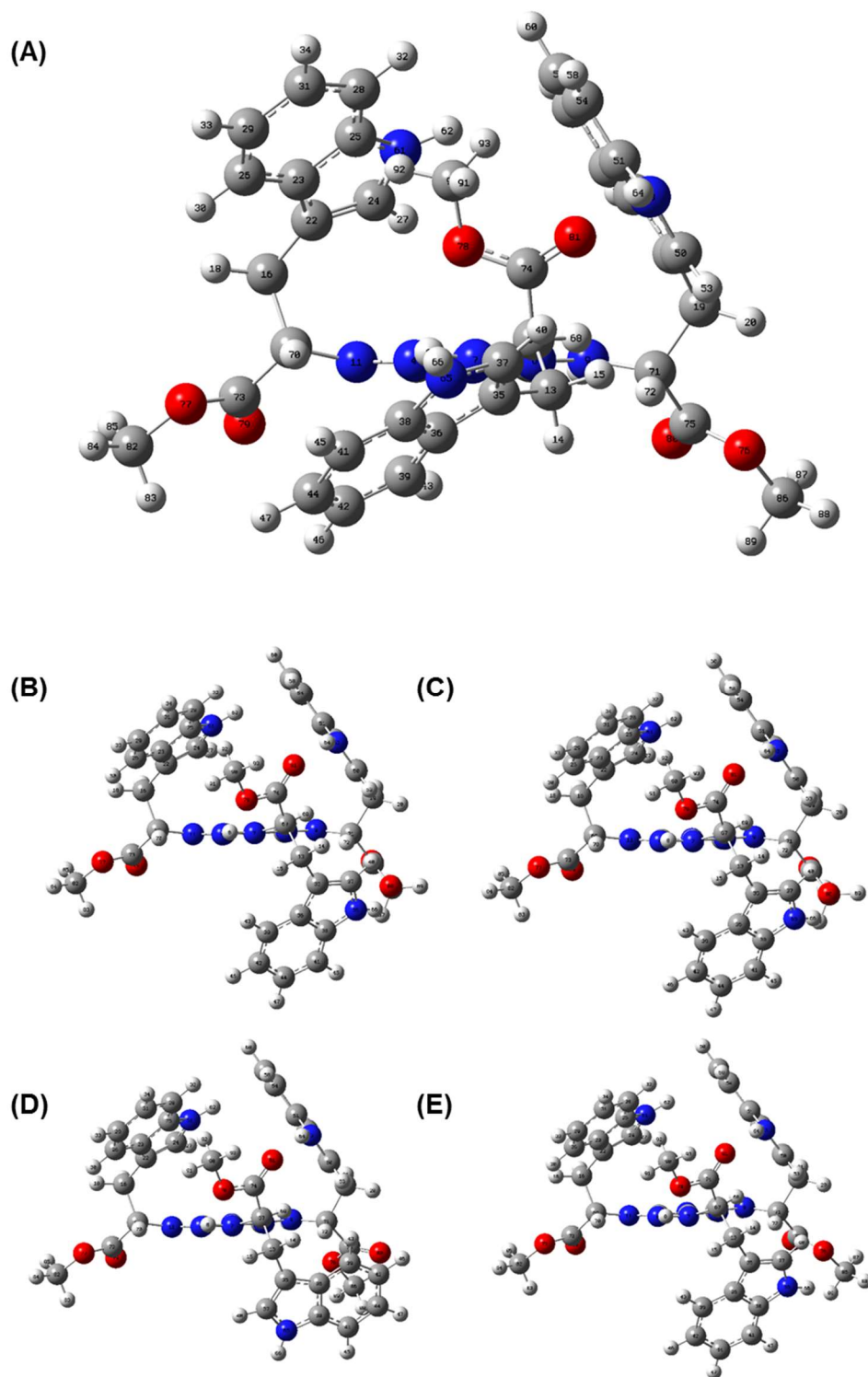
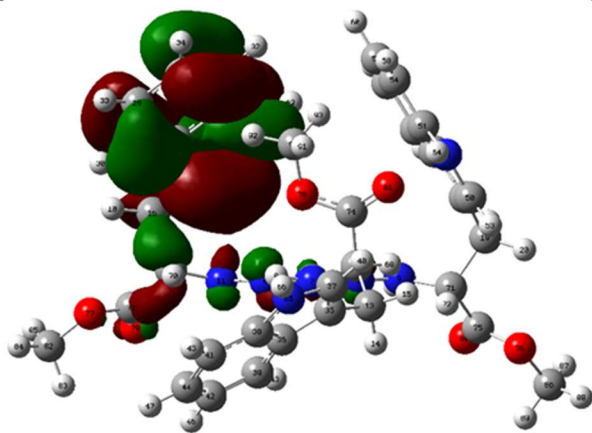


**Figure S20:** First 5 lowest energy conformers obtained after the DFT calculation of W<sub>3</sub>T (arranged in ascending order). Corresponding energies (kJ/mol): (A) -6442586.150 (B) -6442585.719 (C) -6442585.718 (D) -6442581.225 (E) -6442580.497.

(A)



(B)

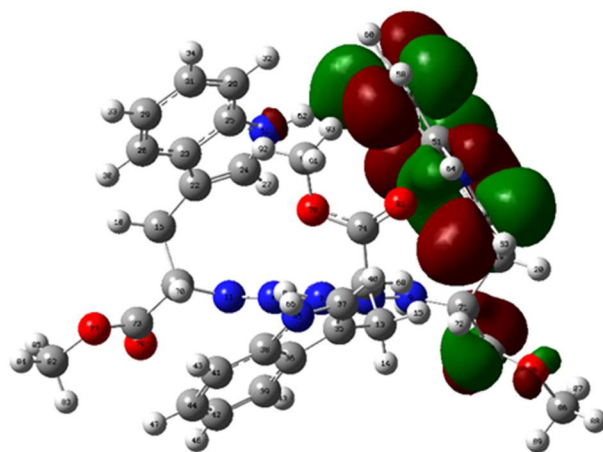
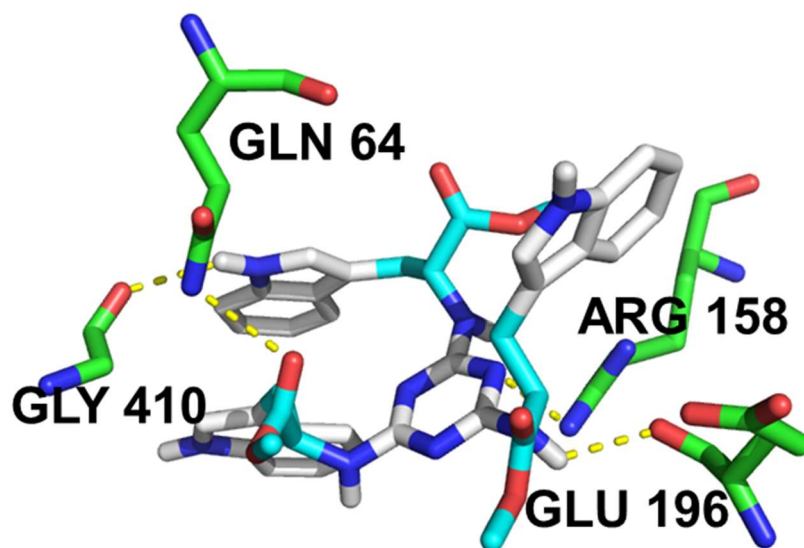


**Figure S21:** HOMO and LUMO molecular orbitals of **W<sub>3</sub>T**.



Triazine Derivative	Binding Affinity (kcal/mol)
<b>W<sub>3</sub>T</b>	<b>- 8.2</b>

**Figure S22.** Molecular docking images of W<sub>3</sub>T and binding affinity of the molecules with tubulin.

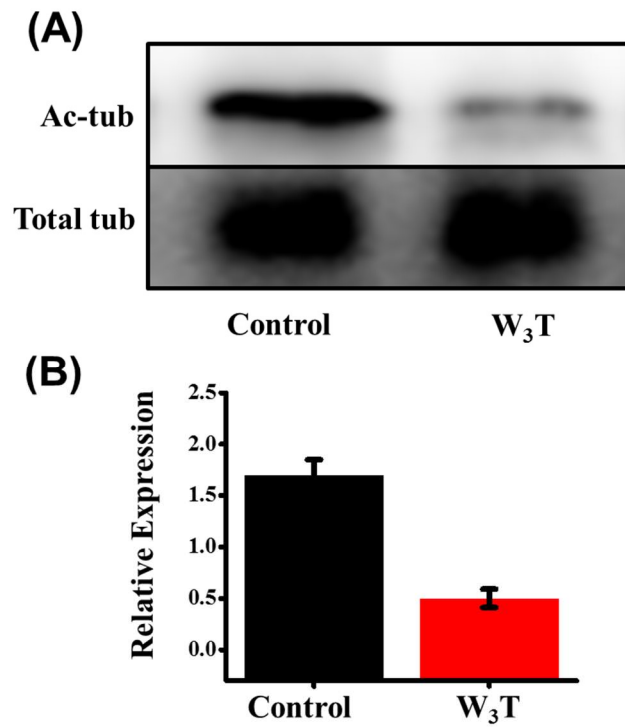


**Figure S23.** (A) Western blots of acetylated tubulin (Ac-K40) with W3T treated as compared to control. (A) Bar diagram of relative expression of acetylated tubulin normalized with loading control.

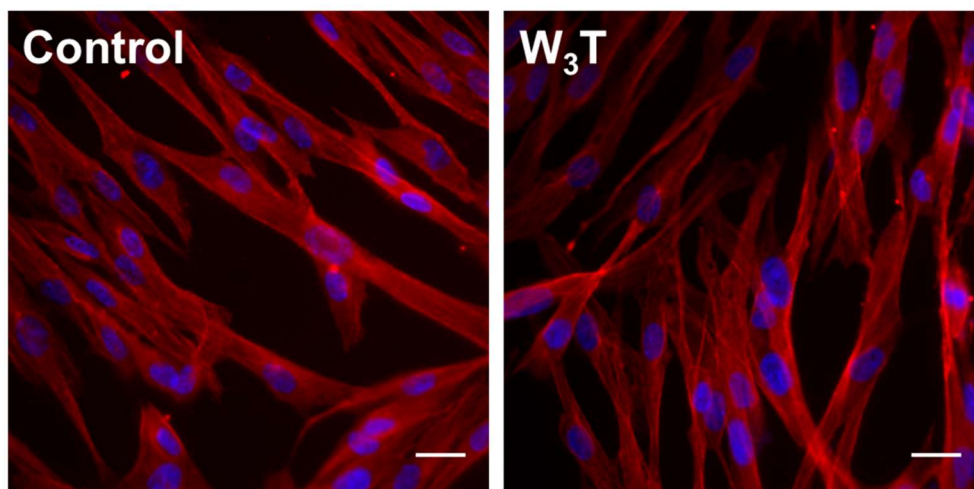


**Figure S24.** Effect of W3T on microtubule networks of WI38 cell lines compared to untreated control.

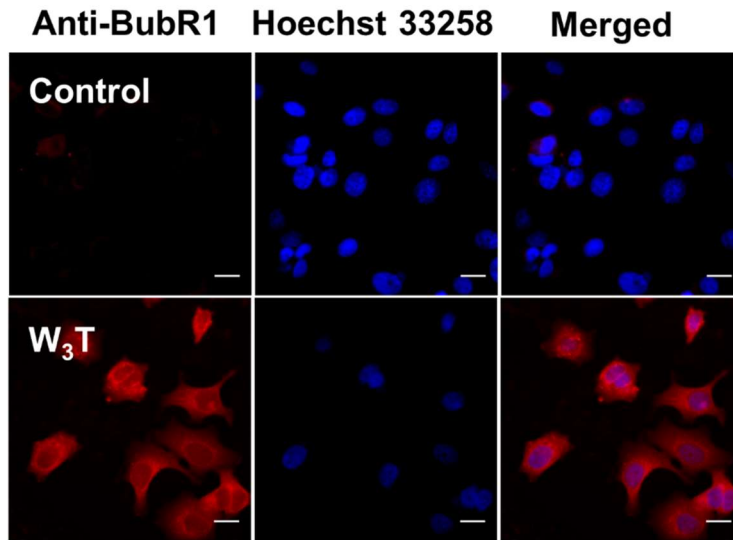


**Figure S25.** Expression of BubR1 after overnight treatment of **W<sub>3</sub>T** is higher compared to untreated control. Immunocytochemistry was performed thrice and it gave similar results. Scale bars correspond to 20  $\mu\text{m}$ .

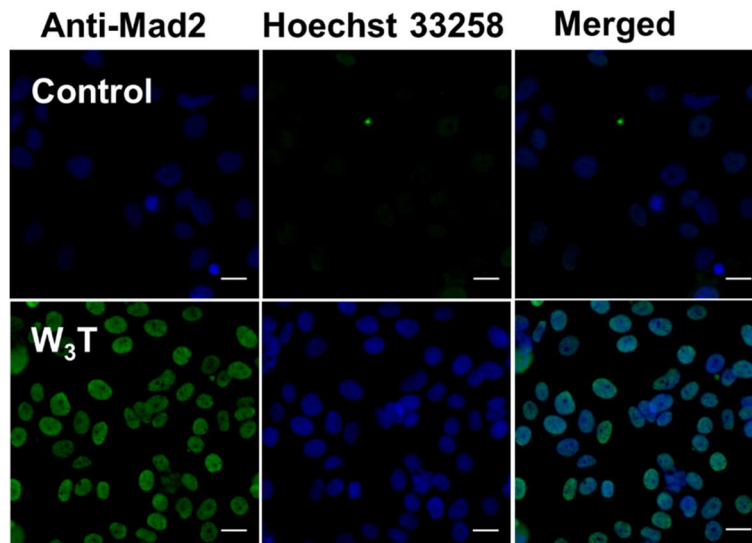


**Figure S26.** Expression of Mad2 is higher after treatment of **W<sub>3</sub>T** compared to untreated control. Immunocytochemistry was performed thrice and it gave similar results. Scale bars correspond to 20  $\mu\text{m}$ .

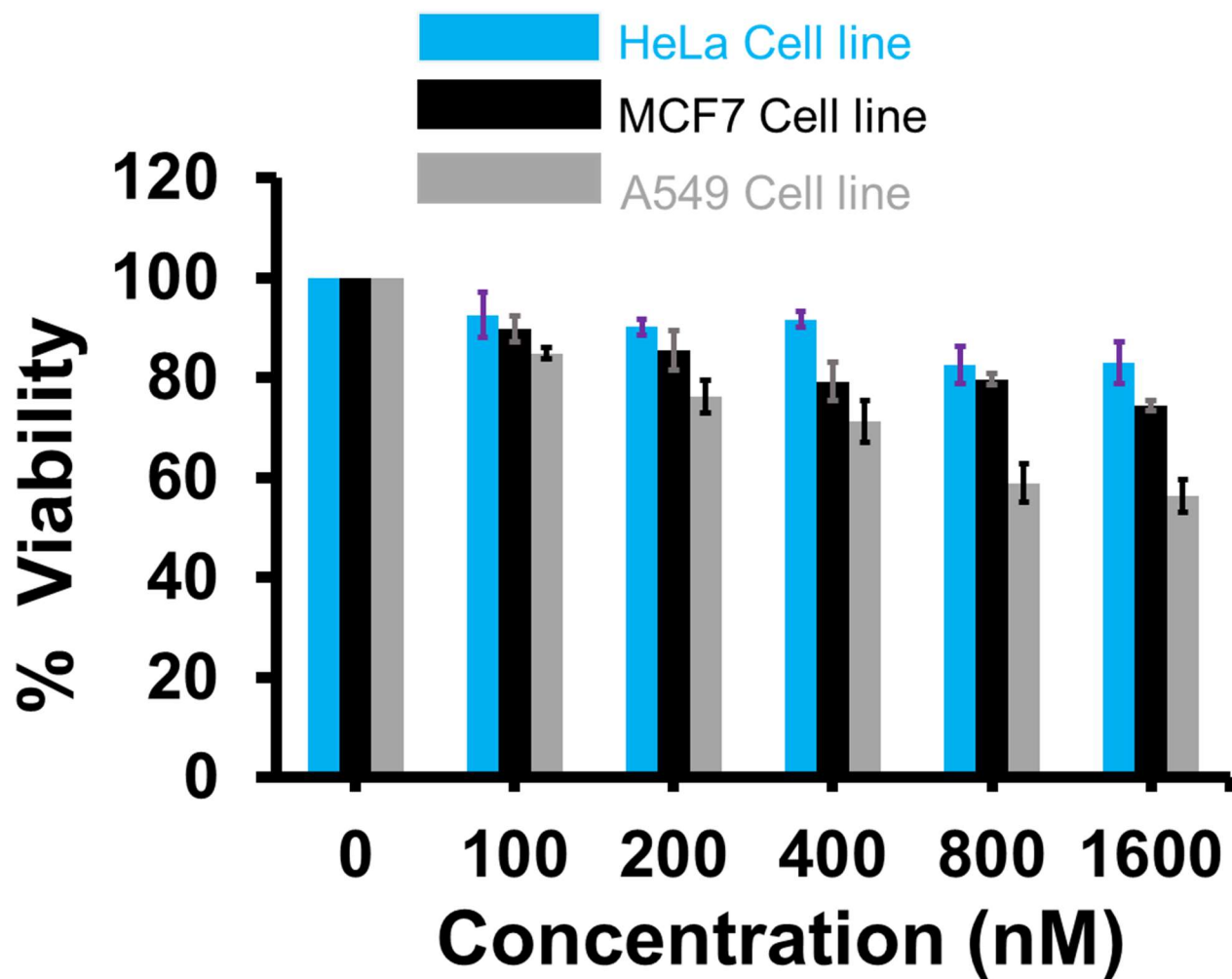


**Figure S27.** Cell viability plots of W<sub>3</sub>T on three different cell lines (HeLa, MCF7 and A549) assessed through MTT assay. MTT assay on all cell lines have been repeated three times. Data shown as mean  $\pm$  S.D.

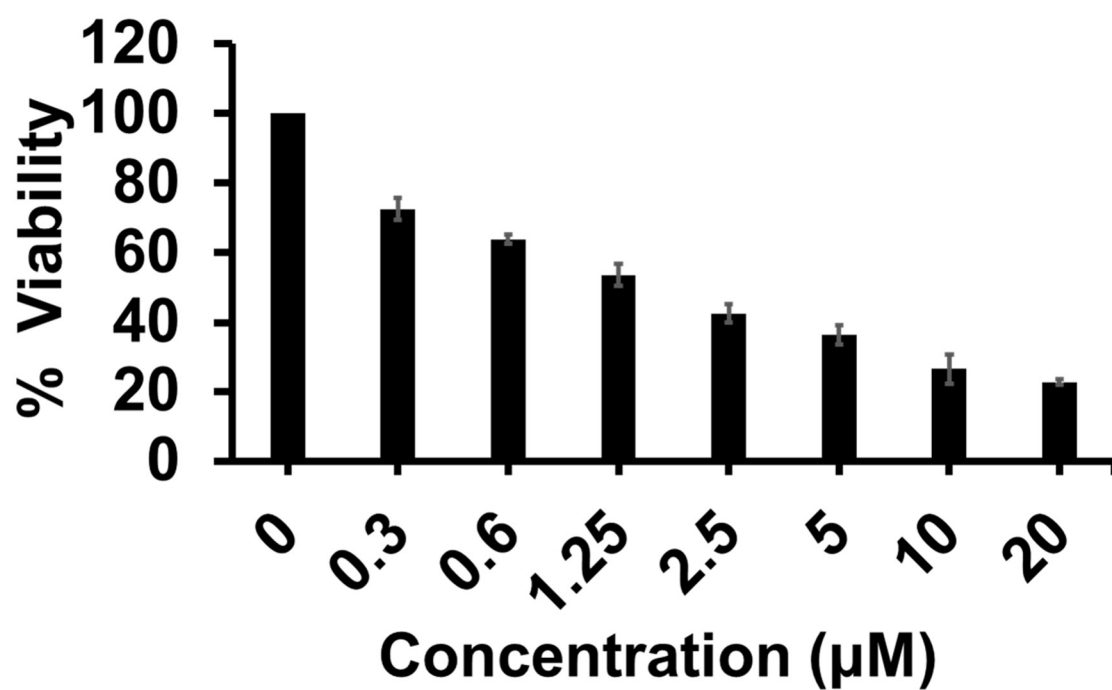


**Figure S28.** Cytotoxicity evaluation of Colchicine as positive control.

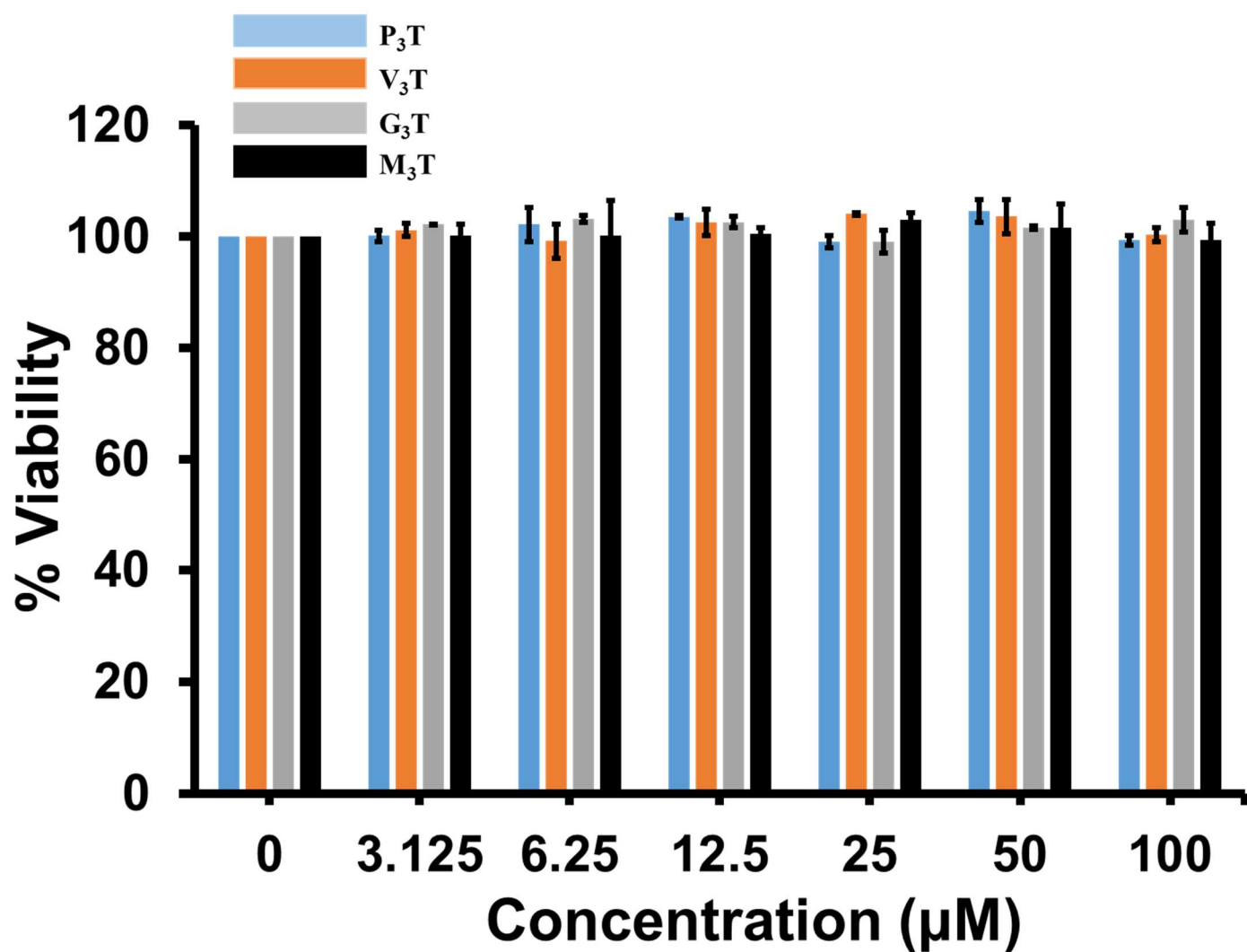


**Figure S29.** Cell cyto-toxicity evaluation of P<sub>3</sub>T, V<sub>3</sub>T, G<sub>3</sub>T and M<sub>3</sub>T in A549 cell line through MTT assay. MTT assay on all cell lines have been repeated three times. Data shown as mean ± S.D.

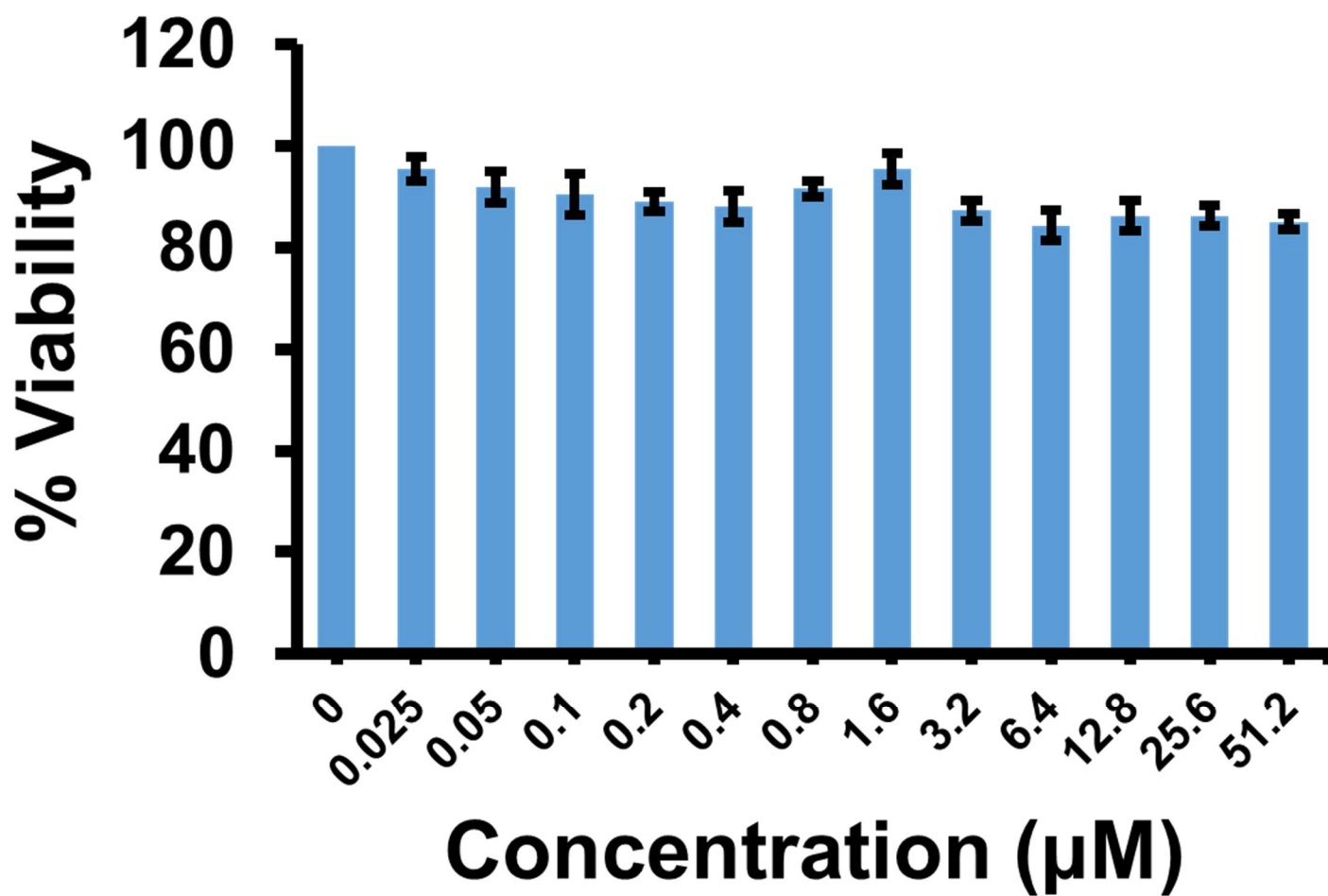


**Figure S30.** Cell viability assay of WI38 cells on treatment with different concentrations of W<sub>3</sub>T through MTT assay. MTT assay on all cell lines have been repeated three times. Data shown as mean ± S.D.

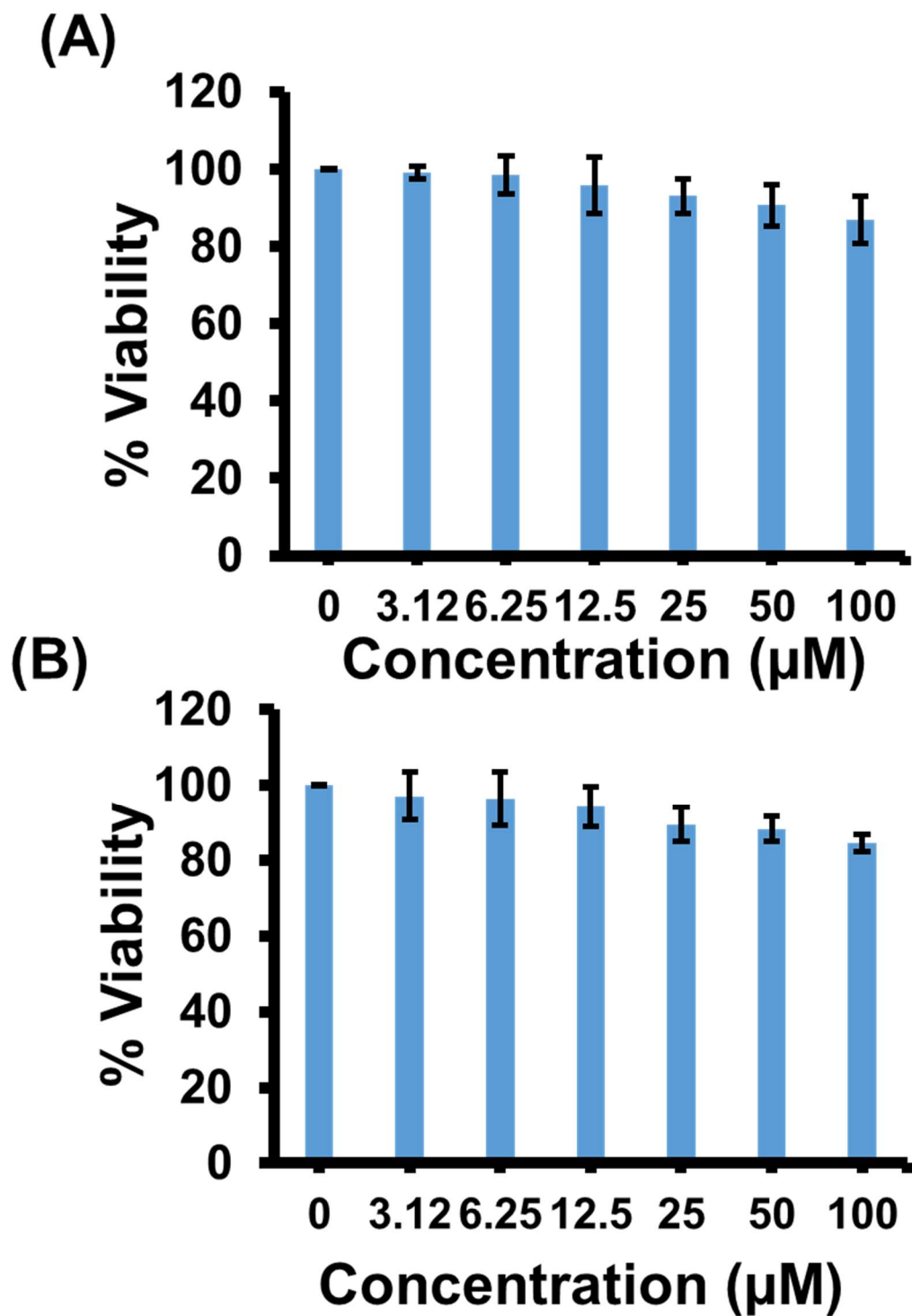


**Figure S31.** Cell viability assay of **W<sub>3</sub>T** on normal cell lines (A) C2C12 and (B) MCF10A through MTT. MTT assay on all cell lines have been repeated three times. Data shown as mean  $\pm$  S.D.

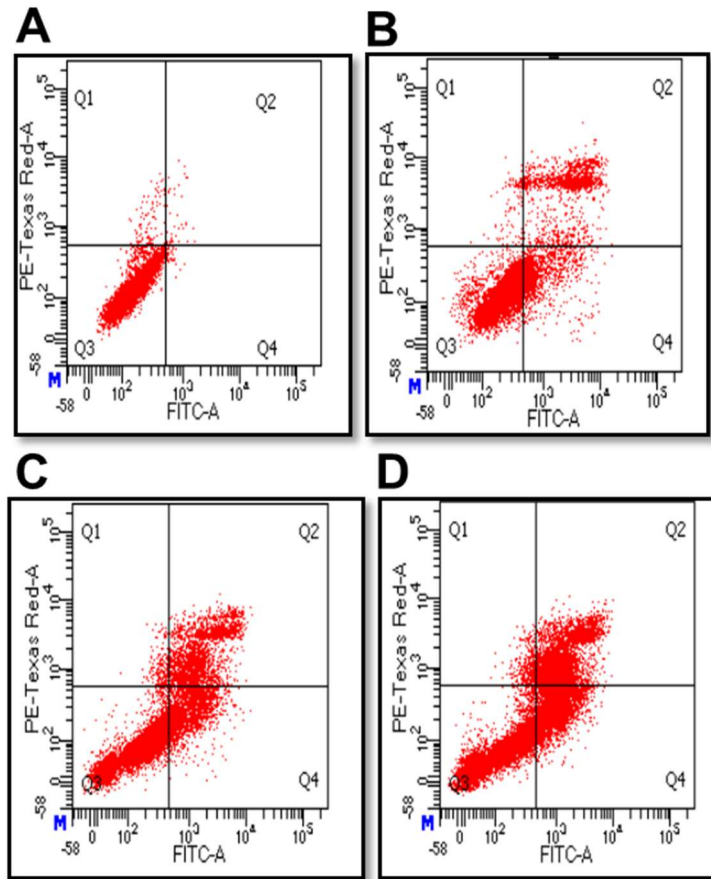


**Figure S32.** Apoptotic death after treatment with W<sub>3</sub>T of A549 cells for Control Experiment (A); Cells were treated with CW (1 μM) (F); Cells were treated with CW (2 μM)(G); Cells were treated with CW (3 μM).

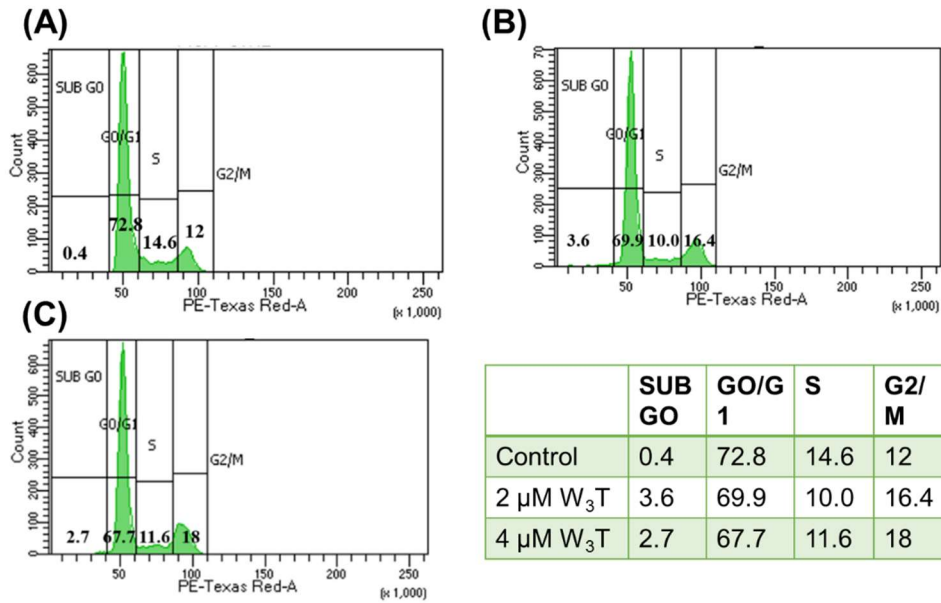


**Figure S33.** Cell cycle study through PI staining of A549 cells in (A) Control untreated cells, (B) on overnight treatment with 2  $\mu$ M of W<sub>3</sub>T and (C) on overnight treatment with 4  $\mu$ M of W<sub>3</sub>T.

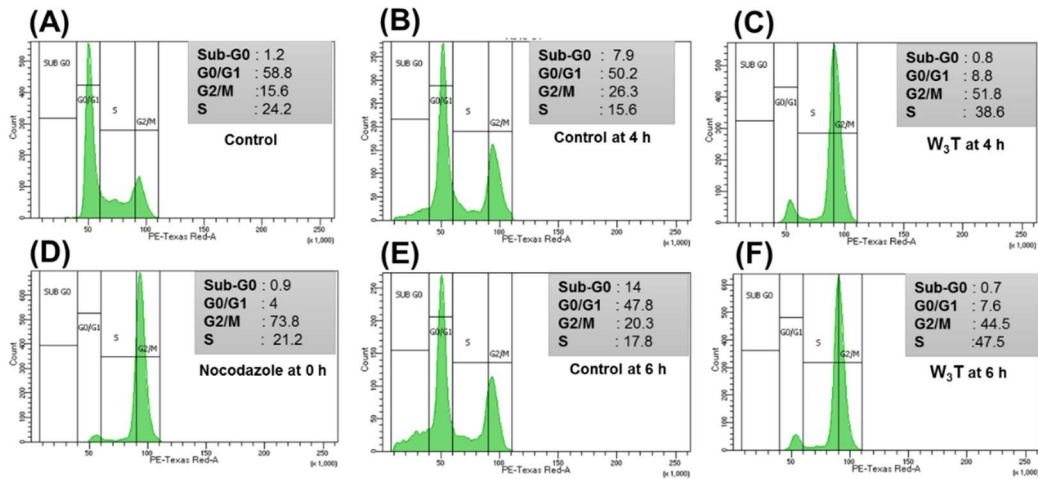


**Figure S34.** W<sub>3</sub>T treatment resulted in delayed mitotic progression in A549 cells. As compared to (A) untreated control A549 cells, (D) A549 cells were treated with 1.3  $\mu$ M Nocodazole which was then washed off and cells were incubated in the absence (B, E) or presence (C, F) of W<sub>3</sub>T for 4 and 6 h and then stained with PI. DNA content was quantified through flow cytometry.

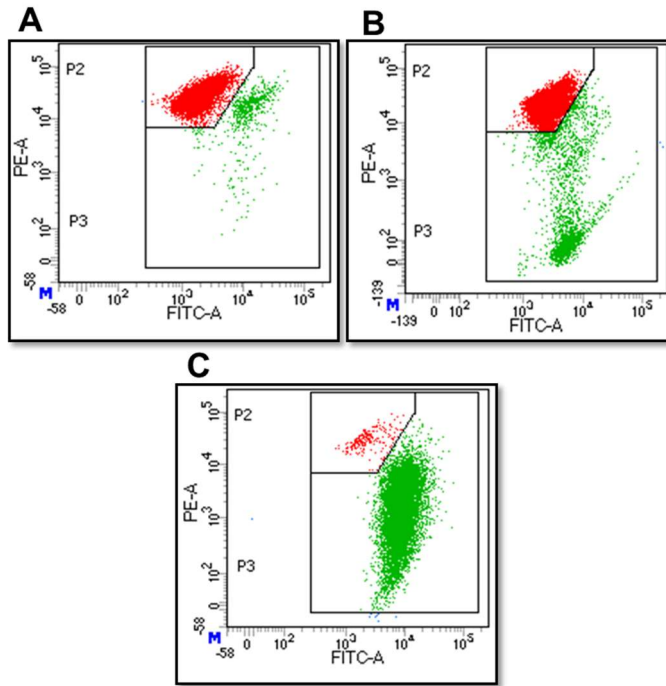


**Figure S35.** JC1 Study of A549 cells for control experiment (A); after treatment with 2  $\mu\text{M}$  CW (B) after treatment with 4  $\mu\text{M}$  CW (C).

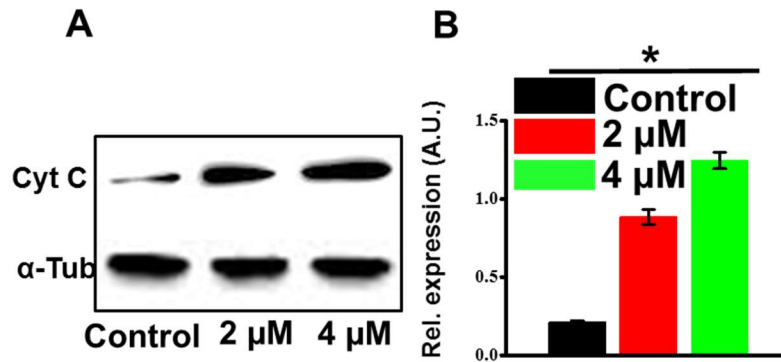


**Figure S36.** Immunoblotting experiment of Cytc in A549 cells after CW treatment as compared to Control (A). Bar diagram of Cytc activation in A549 cells after CW treatment along with control (B).

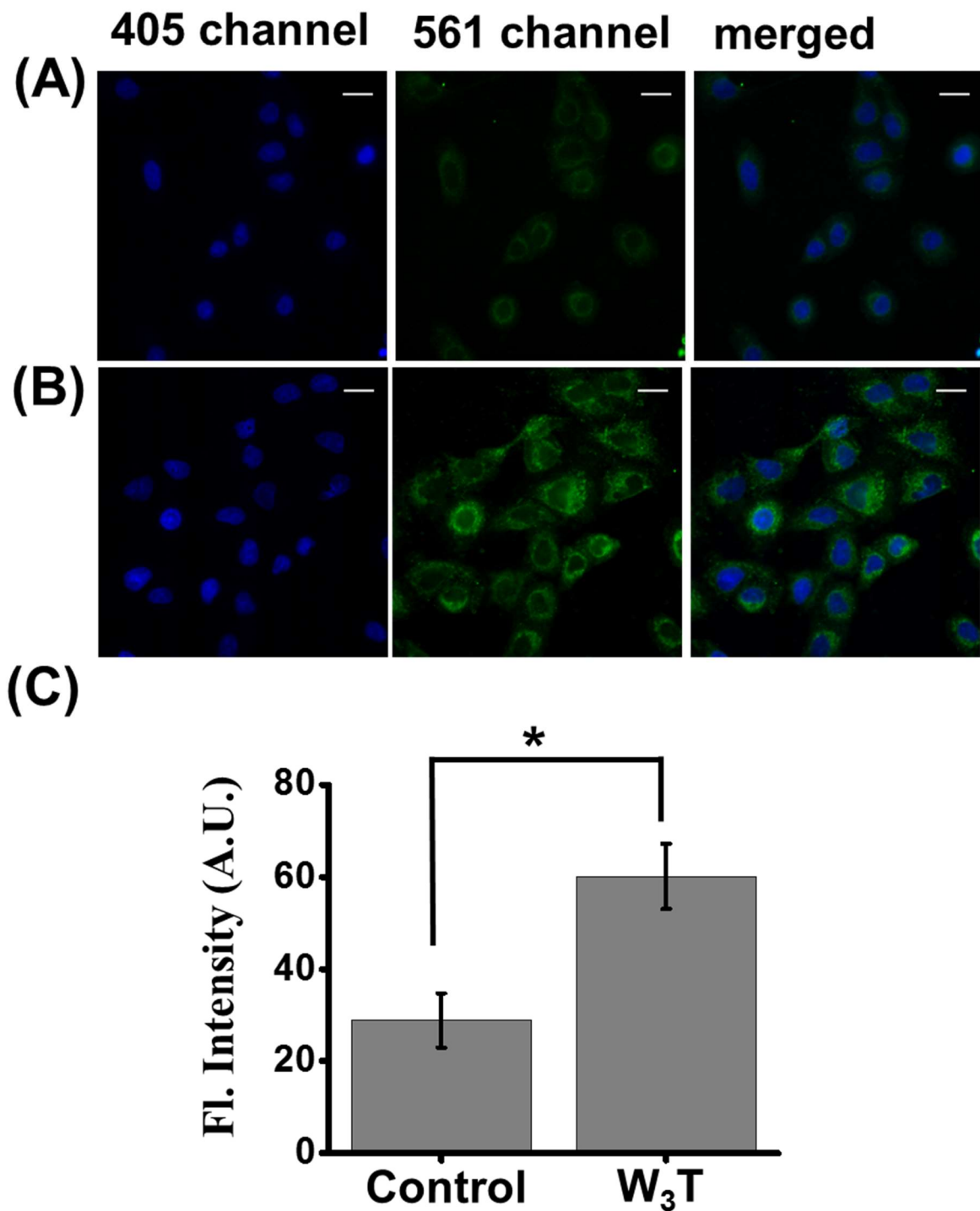


**Figure S37.** Immunocytochemistry experiment shows higher activation of p21 proteins in A549 cells treated with (B) W<sub>3</sub>T as compared to (A) control and (C) Bar diagram showing p21 protein activation in A549 cells after W<sub>3</sub>T treatment. Data shown as mean ±S.D (\*p < 0.05, performing student's t-test). This experiment has been performed thrice and all results obtained similar. Scale bars correspond to 20 μm.

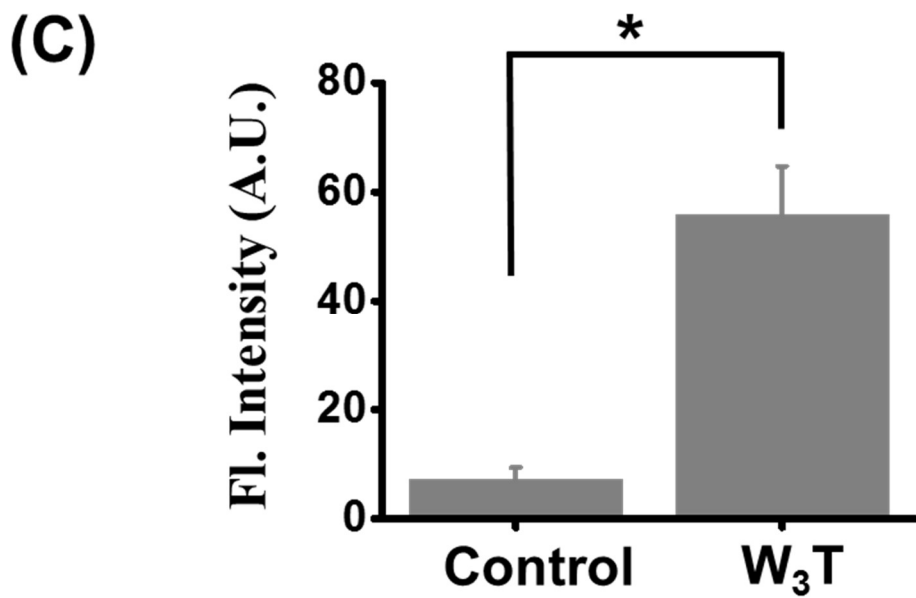
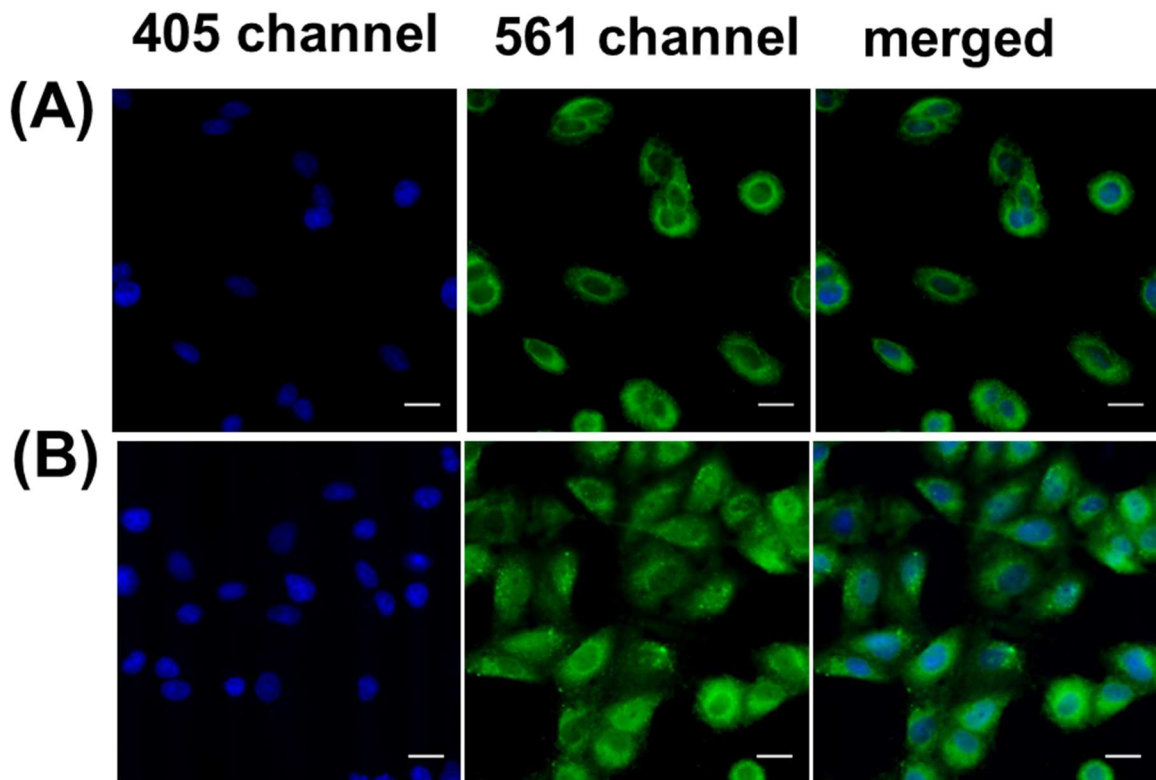


**Figure S38.** Immunocytochemistry experiment shows higher activation of p53 proteins in A549 cells treated with (B) W<sub>3</sub>T as compared to (A) control and (C) Bar diagram showing p53 protein activation in A549 cells after W<sub>3</sub>T treatment. Data shown as mean  $\pm$ S.D (\* $p < 0.05$ , performing student's t-test). This experiment has been performed thrice and all results obtained similar. Scale bars correspond to 20  $\mu$ m.

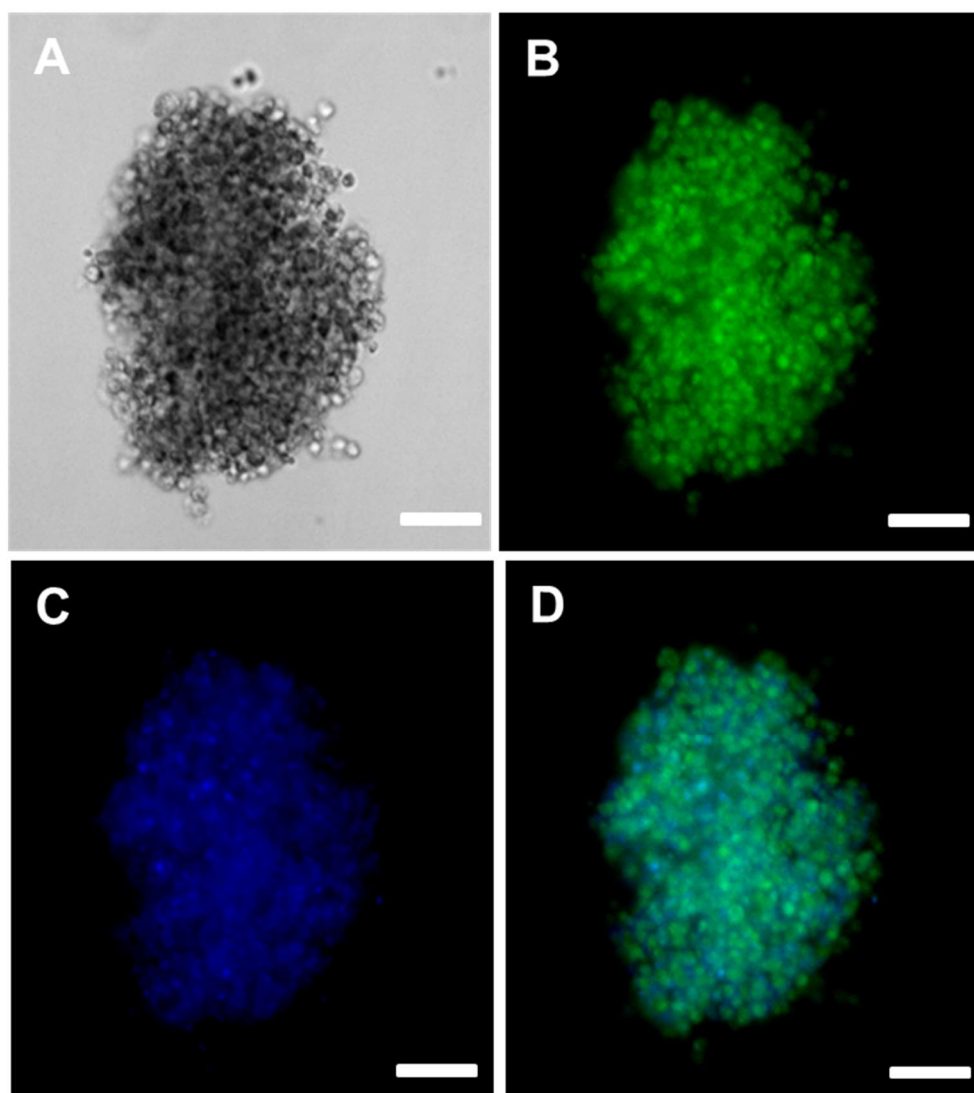


**Figure S39.** Uptake of F-W<sub>3</sub>T in 3D spheroid image in bright field (A); Image in 488 nm channel (B); Image in 405 nm channel(C); merged image of 405 and 488 nm channels (D).

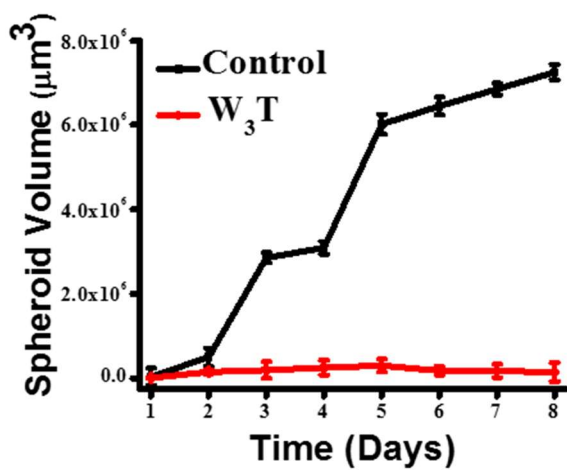
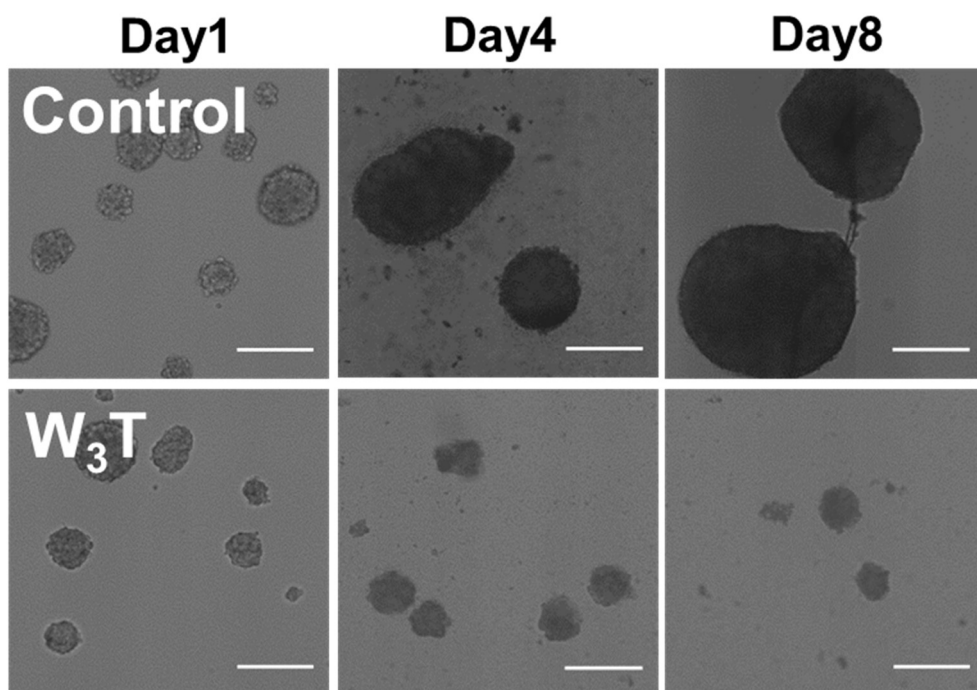


**Figure S40.** Spheroid Growth inhibition after treatment with W<sub>3</sub>T compare to control of A549 cells.

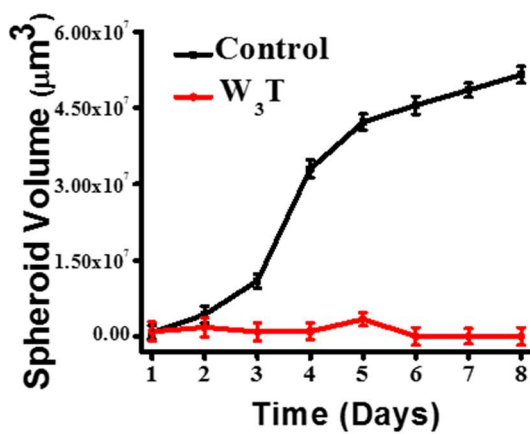
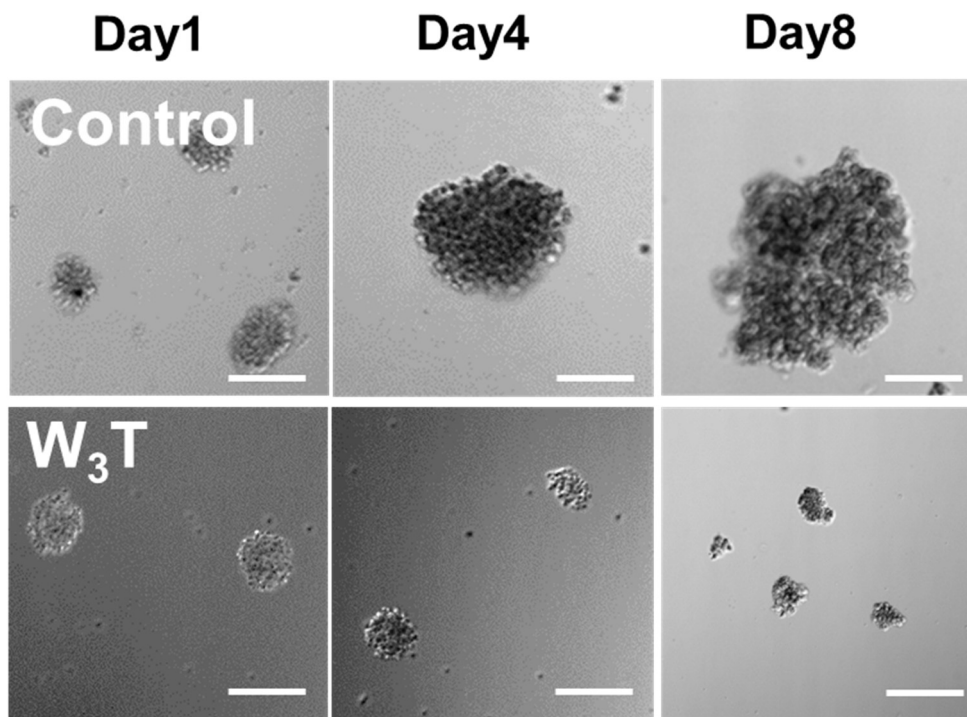


**Figure S41.** Spheroid Growth inhibition after treatment with W<sub>3</sub>T compare to control of B16F10 cells.

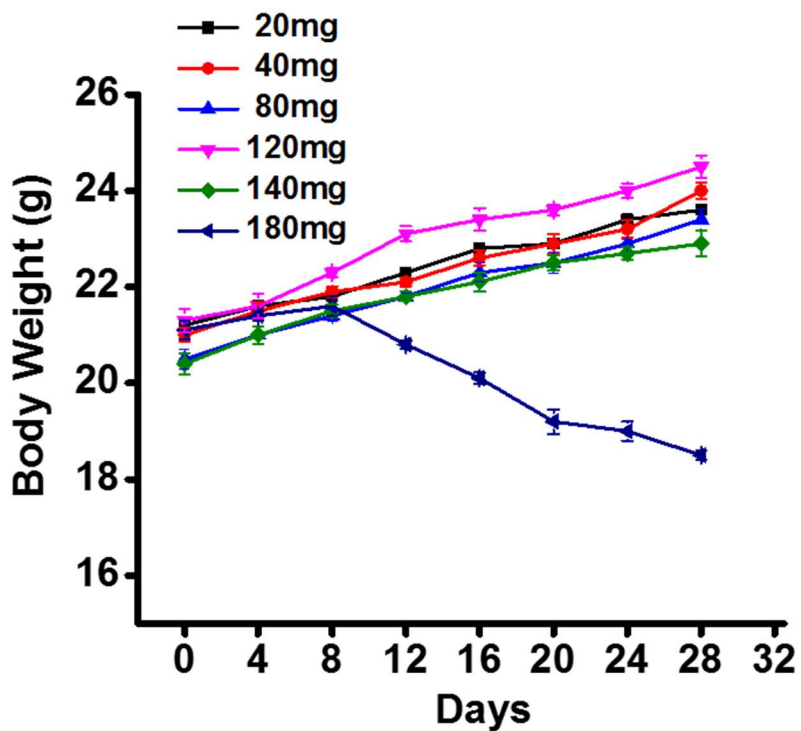


**Figure S42.** The variation of body weight of mice during MTD experiment.

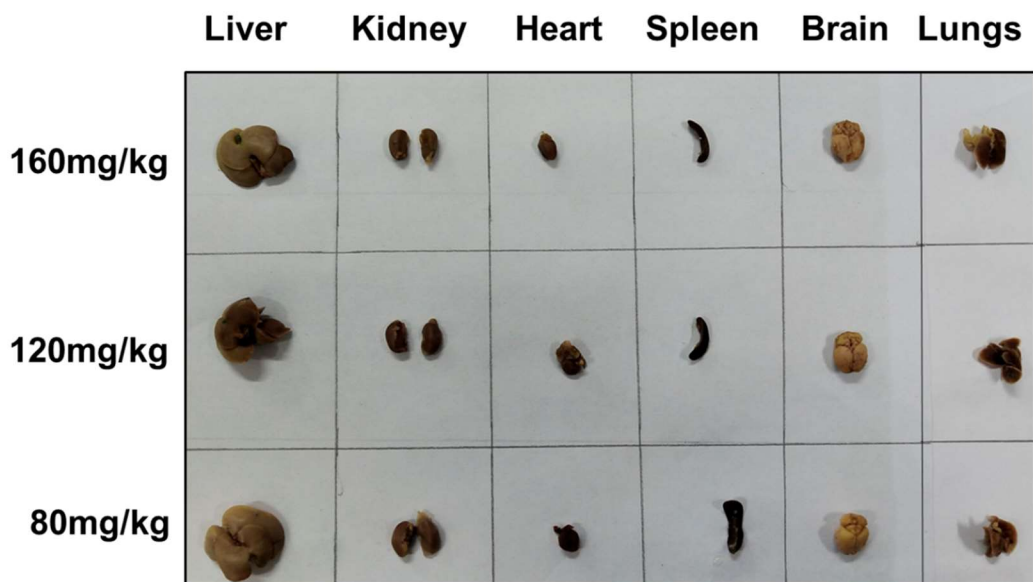


**Figure S43.** The images of various organs after treatment of different doses of W3T.

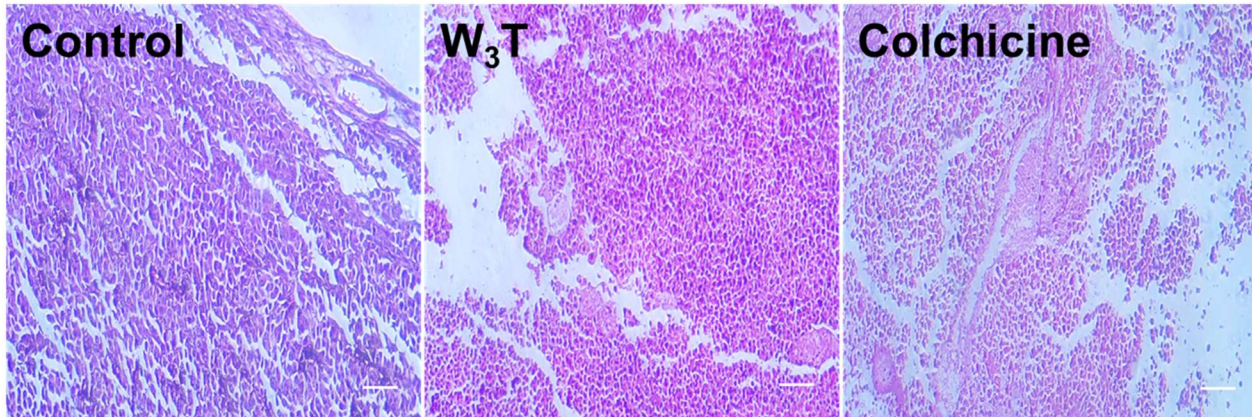


**Figure S44.** Melanoma tumor slices from C57BL/6J mice were stained with hematoxylin and eosin (HE). Images of (A) Tumor slice of control mice and (B) tumor slice of **W<sub>3</sub>T** treated mice taken under a 10X objective. Scale bars correspond to 100  $\mu$ m.

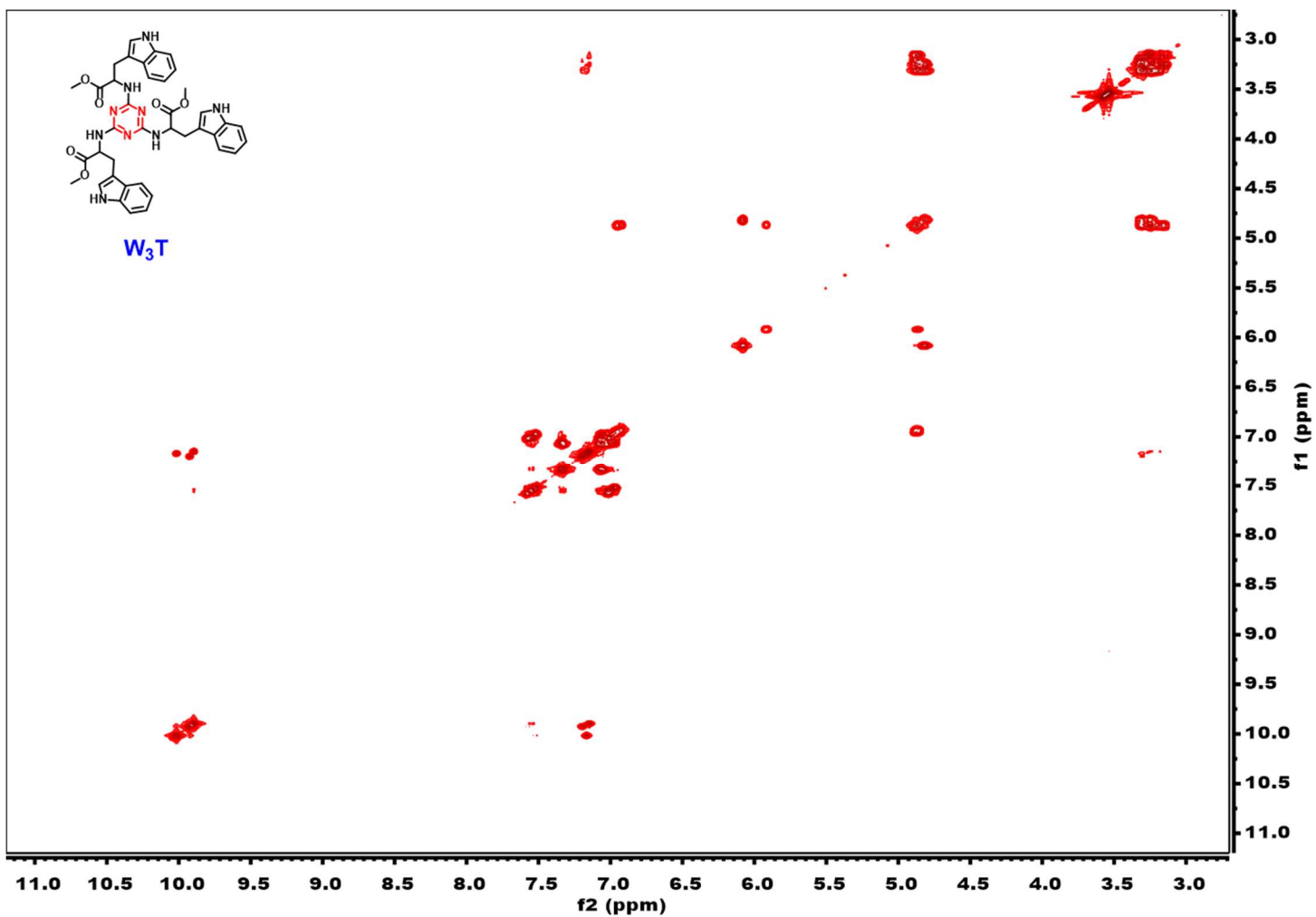
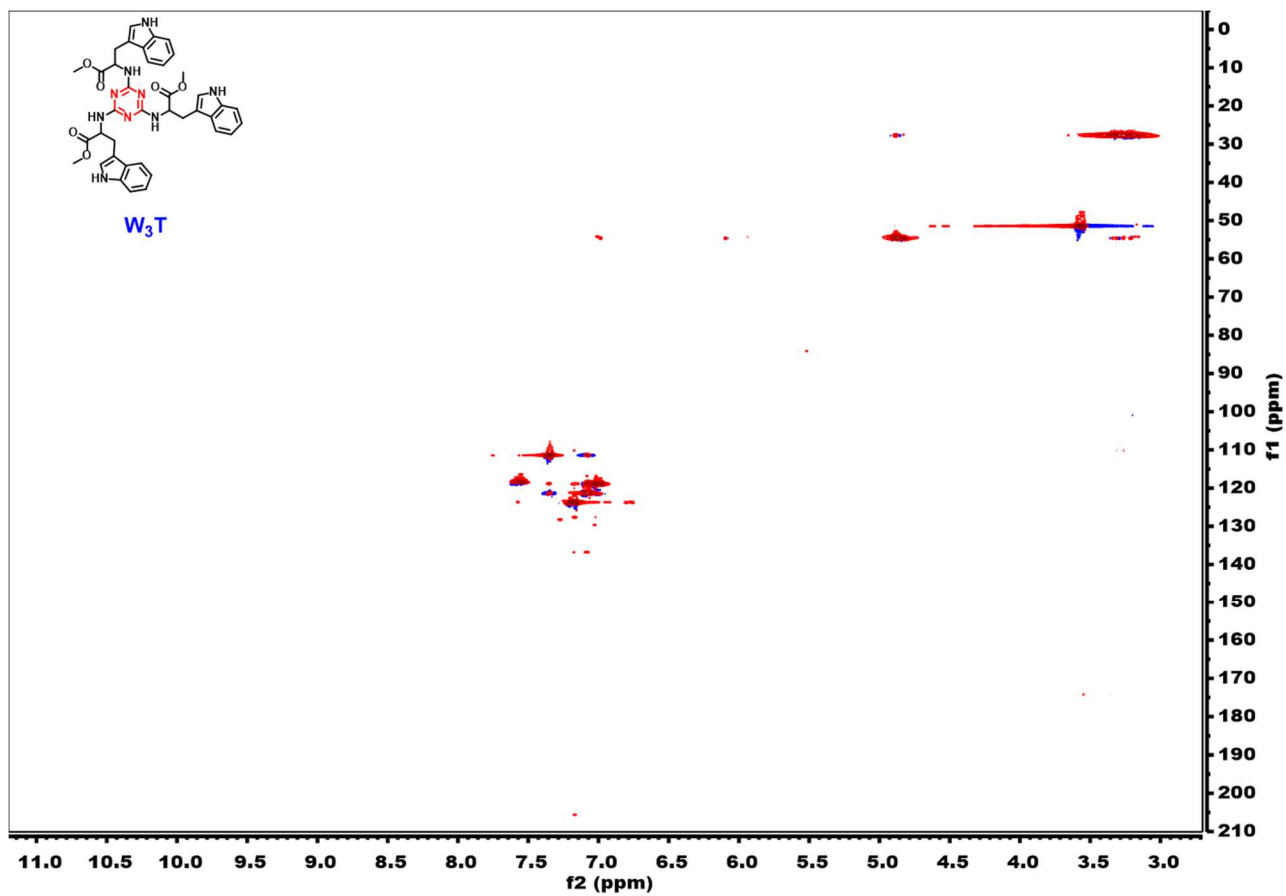


Figure S45. COSY spectrum of W<sub>3</sub>T.



**Figure S46.** HSQC spectrum of **W<sub>3</sub>T**.

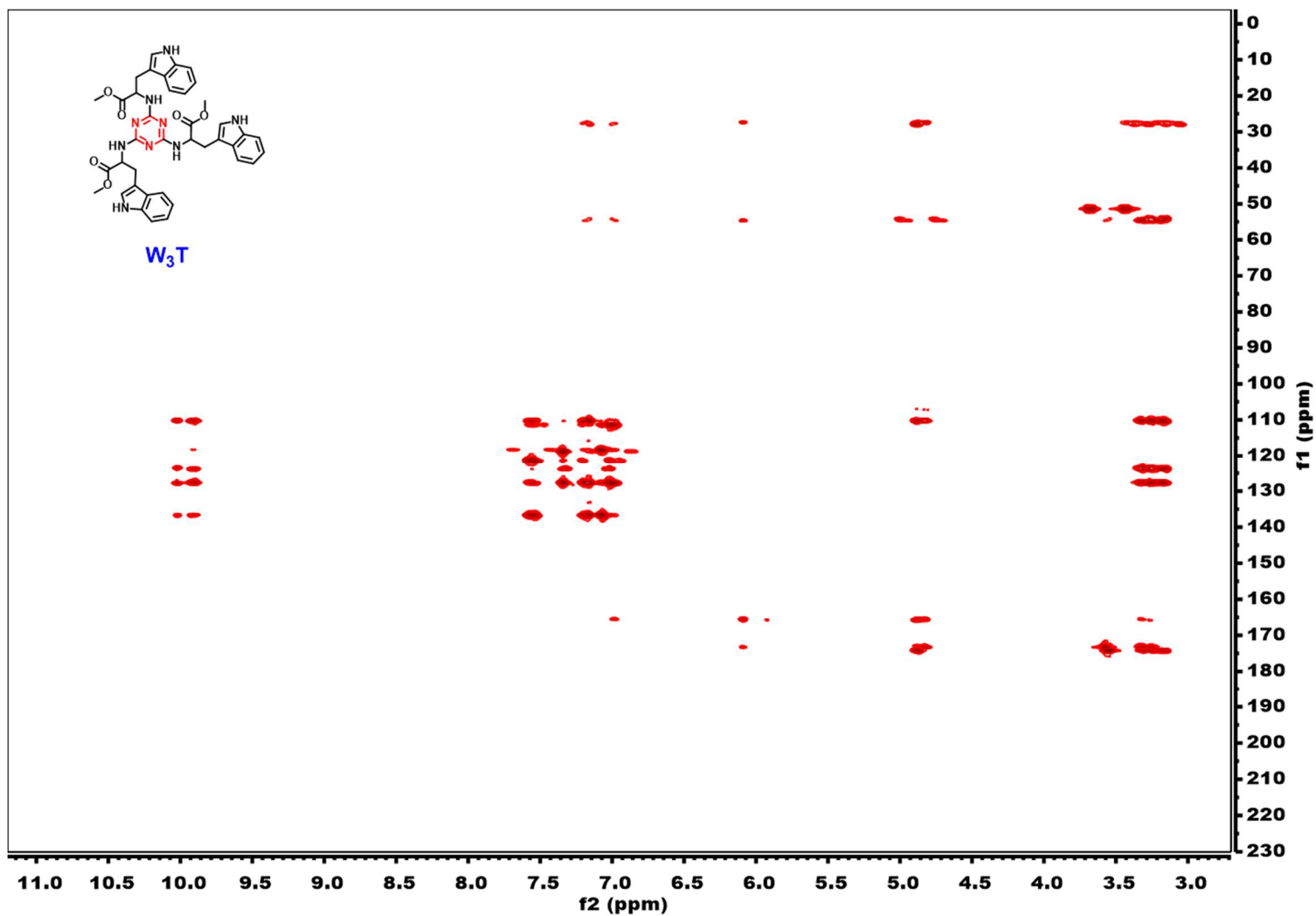


Figure 47. HMBC spectrum of **W<sub>3</sub>T**.

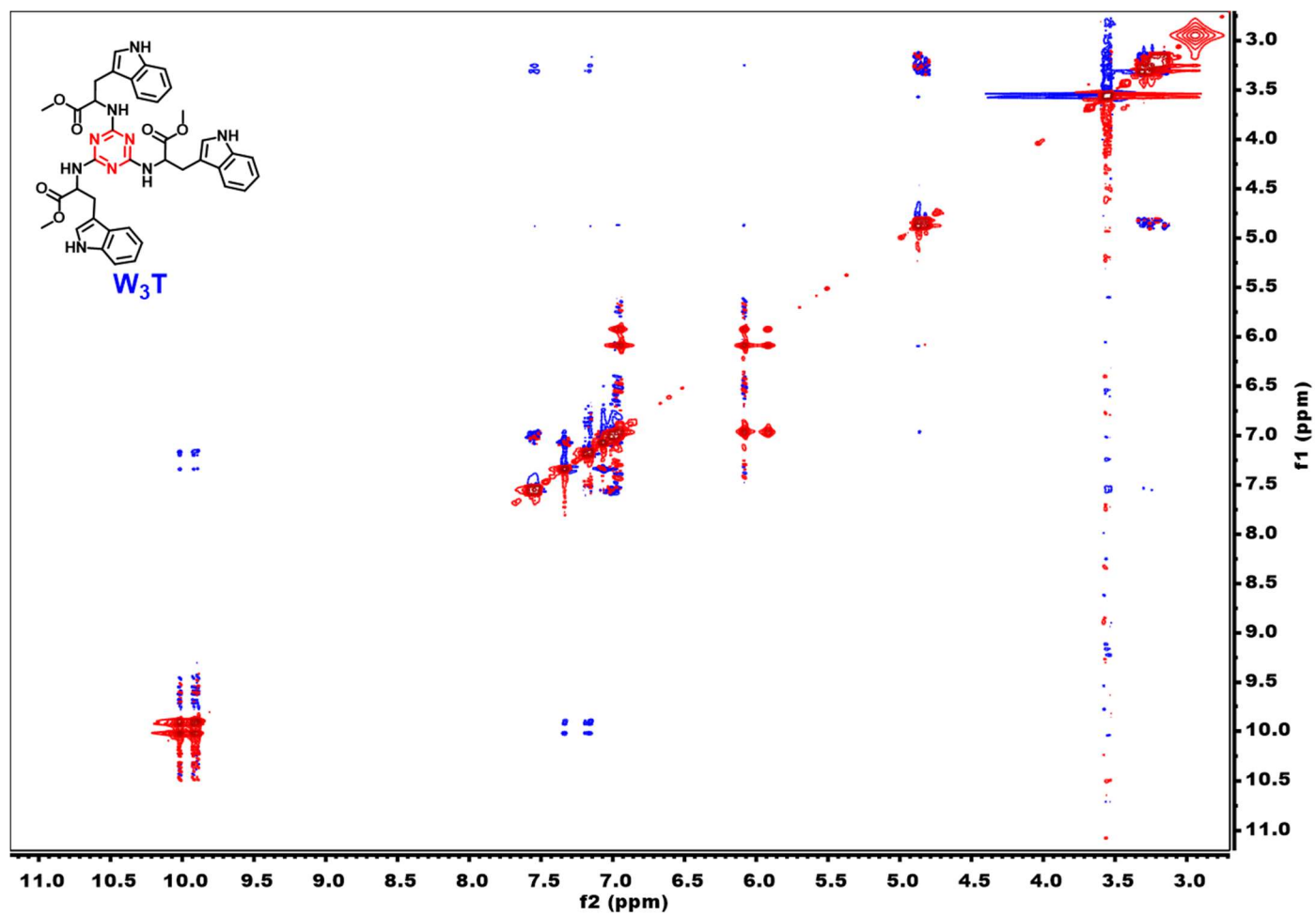


Figure S48. NOESY spectrum of  $W_3T$ .

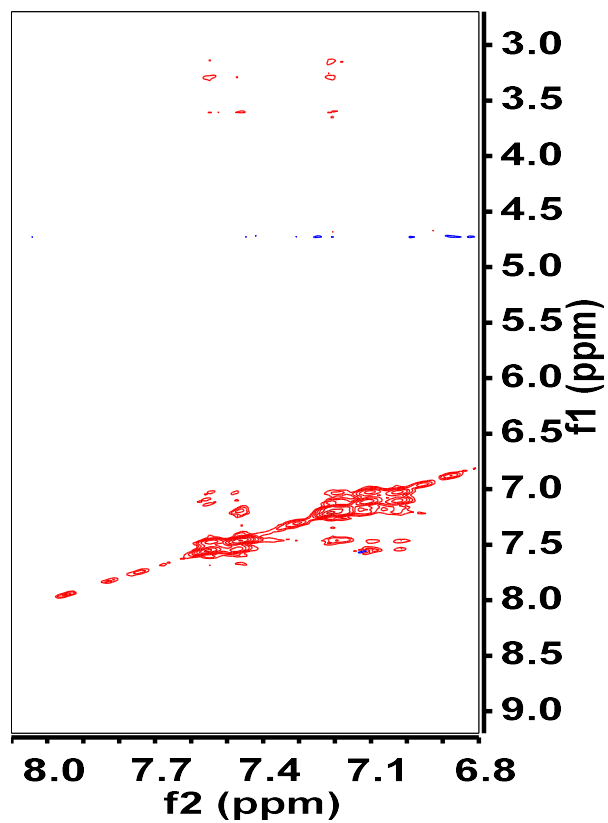


Figure S49. Control TR-NOESY for W<sub>3</sub>T.

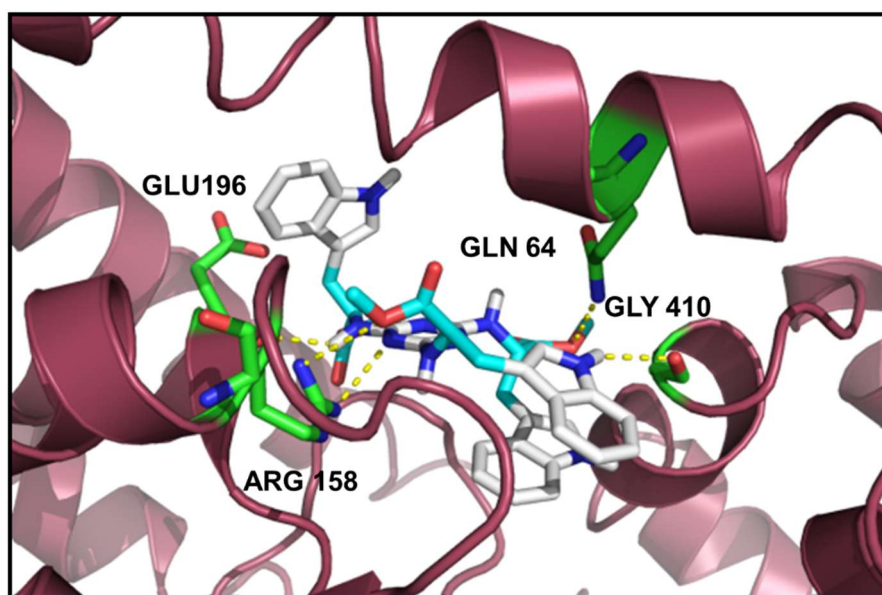


Figure S50: Conformation of W<sub>3</sub>T when binds to microtubule.